การกำจัดแอมโมเนียมและผลิตมวลชีวภาพ โดยไซยาโนแบคทีเรียเซลล์เดี่ยว *Synechococcus* sp.

นางสาวพิรุฬห์พร ศรีมงคล

วิทยานิพนธ์นี้เป็นส่วนหนึ่งของการศึกษาตามหลักสูตรปริญญาวิทยาศาสตรดุษฎีบัณฑิต
สาขาวิชาเทคโนโลยีชีวภาพ
คณะวิทยาศาสตร์ จุฬาลงกรณ์มหาวิทยาลัย
ปีการศึกษา 2560

AMMONIUM REMOVAL AND BIOMASS PRODUCTION BY UNICELLULAR CYANOBACTERIUM *Synechococcus* sp.

Miss Piroonporn Srimongkol

A Dissertation Submitted in Partial Fulfillment of the Requirements
for the Degree of Doctor of Philosophy Program in Biotechnology
Faculty of Science
Chulalongkorn University
Academic Year 2017

Thesis Title	AMMONIUM REMOVAL AND BIOMASS PRODUCTION BY UNICELLULAR CYANOBACTERIUM *Synechococcus* sp.
By	Miss Piroonporn Srimongkol
Field of Study	Biotechnology
Thesis Advisor	Associate Professor Aphichart Karnchanatat, Ph.D.
Thesis Co-Advisor	Associate Professor Nuttha Thongchul, Ph.D.
	Assistant Professor Saranya Phunpruch, Ph.D.

Accepted by the Faculty of Science, Chulalongkorn University in Partial Fulfillment of the Requirements for the Doctoral Degree

.....Dean of the Faculty of Science
(Professor Polkit Sangvanich, Ph.D.)

THESIS COMMITTEE

.....Chairman
(Associate Professor Nattaya Ngamrojanavanich, Ph.D.)

.....Thesis Advisor
(Associate Professor Aphichart Karnchanatat, Ph.D.)

.....Thesis Co-Advisor
(Associate Professor Nuttha Thongchul, Ph.D.)

.....Thesis Co-Advisor
(Assistant Professor Saranya Phunpruch, Ph.D.)

.....Examiner
(Supawin Watcharamul, Ph.D.)

.....Examiner
(Assistant Professor Sanit Piyapattanakorn, Ph.D.)

.....External Examiner
(Chantragan Phiphobmongkol, Ph.D.)

พิรุฬห์พร ศรีมงคล : การกำจัดแอมโมเนียมและผลิตมวลชีวภาพ โดยไซยาโนแบคทีเรียเซลล์เดี่ยว *Synechococcus* sp. (AMMONIUM REMOVAL AND BIOMASS PRODUCTION BY UNICELLULAR CYANOBACTERIUM *Synechococcus* sp.) อ.ที่ปรึกษาวิทยานิพนธ์หลัก: รศ. ดร. อภิชาติ กาญจนทัต, อ.ที่ปรึกษาวิทยานิพนธ์ร่วม: รศ. ดร.ณัฏฐา ทองจุล, ผศ. ดร.สรัญญา พันธุ์พฤกษ์, 72 หน้า.

การเพาะเลี้ยงสาหร่ายขนาดเล็กเพื่อใช้เป็นวัตถุดิบในการผลิตเชื้อเพลิงชีวภาพ ได้รับความสนใจมาเป็นเวลานานกว่าทศวรรษ อย่างไรก็ตามไบโอดีเซลที่ได้จากสาหร่ายก็ยังมีราคาต้นทุนที่สูงกว่าพลังงานรูปแบบอื่นในท้องตลาด ทำให้การผลิตในเชิงพาณิชย์ยังไม่ได้รับความสนใจจากผู้ผลิต อีกทั้งความต้องการใช้น้ำ ซึ่งเป็นปัจจัยหลักในการเพาะเลี้ยงสาหร่ายในปริมาณที่สูงจะส่งผลกระทบต่อภาคการเกษตรในอนาคตหากมีการขยายขนาดเพาะเลี้ยง งานวิจัยนี้มีวัตถุประสงค์เพื่อใช้น้ำทิ้งจากฟาร์มเลี้ยงกุ้งน้ำกร่อยมาเป็นน้ำสำหรับเพาะเลี้ยงสาหร่าย ซึ่งนอกจากจะเป็นการลดต้นทุนแล้วยังสามารถลดปริมาณแอมโมเนียม ซึ่งเป็นของเสียจากการเลี้ยงกุ้งก่อนปล่อยออกสู่สิ่งแวดล้อมอีกด้วย ดังนั้นเพื่อศึกษาปริมาณแอมโมเนียมที่เหมาะสมต่อการเจริญเติบโตของสาหร่าย *Synechococcus* sp. จะถูกเลี้ยงในอาหาร BG-11 ที่เสริมด้วยสารละลาย Turks Island และมีความเข้มข้นของ NH_4Cl ที่ต่างกัน (10-40 mg N L^{-1}) เป็นเวลา 18 วัน ผลการทดลองพบว่า การเจริญของ *Synechococcus* sp. เพิ่มขึ้นในอาหารที่มีความเข้มข้นของแอมโมเนียม 10 mg N L^{-1} ในขณะที่แอมโมเนียมเข้มข้น 20 mg N L^{-1} ขึ้นไป มีผลทำให้การเจริญเติบโตลดลง นอกจากนี้ยังพบว่าค่ากิจกรรมของเอนไซม์ glutamine synthase และ glutamate synthase ลดลงในขณะที่ค่ากิจกรรมของเอนไซม์ glutamate dehydrogenase เพิ่มขึ้น ซึ่งสอดคล้องกับผลของการแสดงออกของยีนที่ควบคุมการสังเคราะห์เอนไซม์ทั้ง 3 ชนิด ที่ถูกตรวจสอบโดยเทคนิค quantitative PCR พบว่า แอมโมเนียมเข้มข้น 20 mg N L^{-1} ขึ้นไป การแสดงออกของยีน *gln*A และ *glt*B จะลดลง ในขณะที่ *gdh*A มีการแสดงออกเพิ่มขึ้น เมื่อเทียบกับชุดควบคุม ผลการศึกษาประสิทธิภาพในการกำจัดแอมโมเนียม พบว่า แอมโมเนียมถูกกำจัดได้ 98% ในวันที่ 6 ของการเพาะเลี้ยงที่ความเข้มข้นของแอมโมเนียม เริ่มต้น 10 mg N L^{-1} จากนั้นศึกษาสภาวะที่เหมาะสมต่อการผลิตชีวมวลของสาหร่ายควบคู่ไปกับการกำจัดแอมโมเนียม โดยเพาะเลี้ยง *Synechococcus* sp. ภายใต้สภาวะที่มีความเข้มข้นของ NH_4Cl ต่างกัน โดยใช้วิธีการตอบสนองของพื้นผิว (RSM) เพื่อสร้างแบบจำลองการคาดการณ์ผลของตัวแปรอิสระ (พีเอช, ปริมาณหัวเชื้อ, ความเข้มข้นของแอมโมเนียม) ผลการศึกษาพบว่า สภาวะที่เหมาะสมคือ ค่าพีเอช 7.4 หัวเชื้อเริ่มต้น 0.15 (OD_{730}) และความเข้มข้นแอมโมเนียม 10.62 mg N L^{-1} ให้ผลการกำจัดแอมโมเนียมและการผลิตชีวมวลสูงสุดเท่ากับ 90% และ 75.5% ตามลำดับ ภายในเจ็ดวัน นอกจากนี้การวิเคราะห์การแสดงออกของยีน glycerol-3-phosphate acyltransferase (GPAT) ด้วยเทคนิค quantitative PCR พบว่าการแสดงออกของยีน GPAT เพิ่มขึ้น 2.87 เท่าเมื่อเทียบกับชุดควบคุม และมีการเพิ่มขึ้นของกรดไขมันไม่อิ่มตัวอย่างมีนัยสำคัญที่ 14.25% นอกจากนี้พบว่า คุณภาพของน้ำมันที่ได้มีค่าซีเทนอยู่ในเกณฑ์มาตรฐาน EN14214 ของสหภาพยุโรป ดังนั้นผลการศึกษาแสดงให้เห็นว่า *Synechococcus* sp. มีศักยภาพในการนำไปใช้สำหรับการบำบัดน้ำเสียและผลิตชีวมวลเพื่อนำมาใช้เป็นวัตถุดิบในการผลิตไบโอดีเซลได้

สาขาวิชา เทคโนโลยีชีวภาพ ลายมือชื่อนิสิต .....

ปีการศึกษา 2560 ลายมือชื่อ อ.ที่ปรึกษาหลัก .....

ลายมือชื่อ อ.ที่ปรึกษาร่วม .....

ลายมือชื่อ อ.ที่ปรึกษาร่วม .....

5672871023 : MAJOR BIOTECHNOLOGY
KEYWORDS:

PIROONPORN SRIMONGKOL: AMMONIUM REMOVAL AND BIOMASS PRODUCTION BY UNICELLULAR CYANOBACTERIUM *Synechococcus* sp.. ADVISOR: ASSOC. PROF. APHICHART KARNCHANATAT, Ph.D., CO-ADVISOR: ASSOC. PROF. NUTTHA THONGCHUL, Ph.D., ASST. PROF. SARANYA PHUNPRUCH, Ph.D., 72 pp.

Using microalgae as a biofuel feedstock has played more attention over a decade. The cultivation of microalgae requires high water use and high initial investment that can make the process still not economically appealing. This study attempted to examine the potential for using brackish shrimp aquaculture effluents as culture medium for algal biomass production. To investigate whether algae could be used to remove ammonium from brackish shrimp aquaculture wastewater, marine cyanobacterium, *Synechococcus* sp. was cultured in BG-11 medium supplemented with Turks Island salt solution and different concentrations of NH_4Cl (10-40 mg N L^{-1}) for 18 days. The results showed that, the cell density of the *Synechococcus* sp. cultures increased in medium containing 10 mg N L^{-1} of NH_4Cl, while ammonium concentrations greater than 20 mg N L^{-1} had a negative effect on growth. Glutamine synthetase and glutamate synthase activities were also examined, and were found to increase with cell density. Meanwhile, glutamate dehydrogenase activity increased in response to high NH_4Cl concentrations (20-40 mg N L^{-1}). The cellular response to ammonium excess was confirmed by measuring gene expression levels using quantitative PCR. Expression of both *gln*A and *glt*B was down-regulated compared with the control, while that of *gdh*A was up-regulated. At an initial concentration of 10 mg N L^{-1}, 98% of the ammonium was removed by day 6 of cultivation. Then, *Synechococcus* sp. was cultured under different conditions in medium containing varying concentrations of NH_4Cl. Response surface methodology (RSM) was then used to build a predictive model of the combined effects of independent variables (pH, inoculum size, ammonium concentration). At the optimum conditions of initial pH 7.4, inoculum size 0.15 (OD_{730}) and ammonium concentration 10.62 mg N L^{-1}, the maximum ammonium removal and biomass production were about 90% and 75.5%, respectively, after seven days of cultivation. Further, analysis of expression of glycerol-3-phosphate acyltransferase (GPAT) gene by quantitative PCR revealed that transcripts of GPAT were up-regulated by 2.87-folds with a significant increase in unsaturated fatty acid of 14.25% under optimal conditions. The result of biodiesel quality, in terms of cetane number almost attained the European Standards EN14214 criteria; hence, this strain shows promise for use in biodiesel production. Overall results indicate that *Synechococcus* sp. has the potential for use for concurrent water treatment and production of biomass that can be applied for biodiesel feedstock.

Field of Study: Biotechnology
Academic Year: 2017

Student's Signature .....
Advisor's Signature .....
Co-Advisor's Signature .....
Co-Adv sor's Signature .....

ACKNOWLEDGEMENTS

First of all, I would like to express the appreciation to my advisor, Associate Professor Dr. Aphichart Karnchanatat, who gives me an opportunity to do this doctoral research, guidance and support to publish articles from this research work and also in thesis writing. He not only gave me valuable suggestions about my research work but also endowed me with the autonomy of pursuing my ideas. I feel extremely lucky to have an advisor like him and could not have imagined having a better advisor for my doctoral study. Without him, my doctoral research would not have seen the light of the day.

Besides my advisor, I also would like to specifically thank to my co-advisor, Associate Professor Dr. Nuttha Tongchul and Assistant Professor Dr. Saranya Phunpruch, for constant support, encouragement and constructive suggestions.

I express my thanks to the members of my dissertation committee, Associate Professor Dr. Nattaya Ngamrojanavanich, Assistant Professor Dr. Sanit Piyapattanakorn, Dr. Supawin Watcharamul and Dr. Chantragan Phiphobmongkol for their insightful comments and professional guidance.

I would like to acknowledge the Graduate School and Program in Biotechnology, Faculty of Science, Chulalongkorn University, for 60/40 Tuition Fee Scholarship.

I also would like to thank Institute of Biotechnology and Genetic Engineering (IBGE), Chulalongkorn University for support equipment facilities during my experiments.

I am highly thankful to all my colleagues at IBGE, especially, Dr. Tanatorn Saisavoey and Miss Papassara Sangtanoo for being supportive and helpful all the time.

Finally, I must express my very profound gratitude to my family for providing me with unconditional love, support and continuous encouragement throughout my years of study and through the process of researching and writing this thesis. This accomplishment would not have been possible without them. Thank you very much.

CONTENTS

Page

Page

LIST OF TABLES

LIST OF FIGURES

LIST OF ABBREVIATION

A, Abs	Abstract
ANOVA	Analysis of variance
AMT	Ammonium Transporter family
APHA	American Public Health Association
ATP	Adenosine triphosphate
bp	base pair
BOD	Biological oxygen demand (mg L^{-1})
CCD	Central composite design
cDNA	Complementary DNA
CN	Cetane number
COD	Chemical oxygen demand (mg L^{-1})
CPO	crude palm oil
DAG	Diacyl glycerol
DGAT	Diacylglycerol O-acyltransferase
DU	Degree of saturation
Eq	Equation
GC-MS	Gas chromatograph mass spectroscopy
GDH	Glutamate Dehydrogenase
GOGAT	Glutamate Synthase
GPAT	Glycerol-3-phosphate acyltransferase

GS	Glutamine synthetase
G-3-P	Glycerol-3- phosphate
FAME	Fatty acid methyl ester
FAS	Fatty acid synthase
FAO	Food and Agriculture Organization of the United Nations
FFA	Free fatty acid
FFD	Full factorial design
KCl	Potassium chloride
LPAT	Lysophosphatidyl acyltransferas
LPG	Liquid petroleum gas
mg	Miligram
min	Minute
mL	Milliliter
mM	Millimolar
NaCl	Sodium chloride
NADH	Nicotinamide adenine dinucleotide hydride
NaOH	Sodium hydroxide
NH_3	Ammonia
NH_3-N	Ammonia nitrogen
NH_4	Ammonium
NH_4^+	Ammonium ion
NH_4-N	Ammonium nitrogen

NH_4Cl	Ammonium chloride
NO_2-N	Nitrite nitrogen
OD	Optical Density
PAP	Phosphatidic acid phosphatase
qPCR	Quantitative polymerase chain reaction
RBDPO	Refined bleached deodorized palm oil
RNA	Ribonucleic acid
Rnase P	Ribonuclease P
RSM	Response surface methodology
SPSS	Statistical Package for Social Sciences
TAG	Triacylglycerol
TAN	Total ammonium nitrogen
TKN	Total Kjeldahl nitrogen
TP	Total phosphorus

CHAPTER I
INTRODUCTION

The demand for energy is increasing continuously because of increases in population and industrialization. Most energy comes from fossil fuels such as coal, petroleum oil and natural gas, which are non-renewable resource. Therefore, finding alternative sources of energy has attracted attention. The potential for use of algae as a source of renewable energy has received considerable interest because they have many significant advantages (Zhang *et al*., 2016), including a rapid growth rate, high lipid content and the ability to grow without using arable land. Moreover, algae can effectively capture carbon dioxide through photosynthesis and produce polysaccharides and triacylglycerol (TAG). These compounds are the raw materials for production of bioethanol and biodiesel, which can be used in current engines without major modifications (Pulz and Gross, 2004; Vassilev and Vassileva 2016). However, the cultivation of microalgae requires large amounts of water and high initial investments. Therefore, microalgae culture coupled with wastewater treatment is considered one of the most promising routes to overcome these problems because it enables environmentally friendly and cost-effective production of biofuel.

Worldwide, many studies have shown that aquaculture production impacts the environment (Sara, 2007). Especially, ammonium contamination from untreated water causes both environmental and health issues, including eutrophication and toxic effects on aquatic life (Li *et al*., 2007). Thailand is one of the top 15 producers in the aquaculture industry worldwide, and is the largest exporter of crustaceans in South-East Asia (FAO, 2014). A significant problem associated with the growing aquaculture industry is the high quantity of nitrogenous waste that is produced during protein metabolism by the animals, and from the decomposition of nutrients in the aquaculture ponds. Ammonium levels in aquaculture

effluent can vary widely, even in aquaculture source waters. However, levels are generally in the range of approximately 1-10 mg L^{-1} (Chiu-Mei *et al*., 2016; Gustavo *et al*., 2006).

Marine cyanobacteria belonging to the genus *Synechococcus* are some of the most abundant picoplanktonic photoautotrophs in the world's oceans, and are capable of fulfilling their nitrogen requirements using nitrate, ammonia, or in some cases, urea. *Synechococcus* species also have the ability to adapt to a variety of nutrient concentrations and temperatures (Ting *et al*., 2002; Mella-Flores *et al*., 2012). Recently, *Synechococcus* species have been used as a model for synthetic biology studies, with numerous biotechnological applications including various bioactive compounds (Alka and Jayashree, 2010) and production of biofuels (Anne, 2014; McNeely *et al*., 2010).

Although, algae-based biofuel production coupled to bioremediation has been studied for over decade, most algal strains investigated have been from freshwater environments, and thus there is limited information available regarding the ammonium tolerance of algae in saline/brackish water. Thereby, this study aimed to investigate the optimal condition of media for enhancement of algal biomass production together with ammonium removal by *Synechococcus sp.* cultivated in the presence of different levels of ammonium using Response Surface Methodology (RSM) based on Central Composite design (CCD), as well as characterize the fatty acid profile.

CHAPTER II
LITERATURE REVIEW

2.1 Biofuel in Thailand

Thailand has few of its own oil reserves, and thus has to rely overwhelmingly on imported crude oil and petroleum products. In year 2008, out of 47,741 kilo-tonnes of oil used in the country, about 75.1% was imported from overseas. The total value of crude oil imported was $US 34.8 billion (Limanond, Jomnonkwao, & Srikaew, 2011). Thailand's primary fuel consumption is mostly from Diesel, accounting for over 45 percent of the most commonly used, followed by benzene and gasohol, LPG, Jet fuel and residual fuel, respectively (EPPO, 2016) **(Figure 1)**.

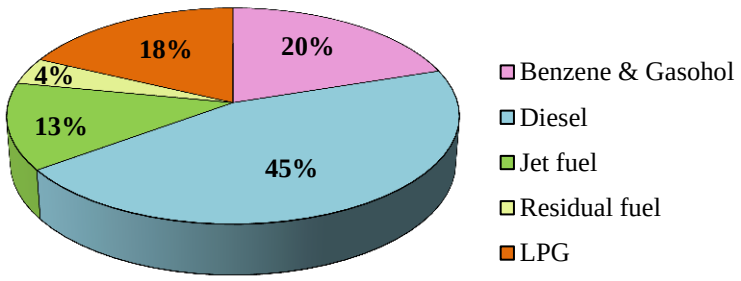

Figure 1 Total fuel consumption in Thailand, 2015

Biofuels in Thailand can be split into two generalized categories as biodiesel and ethanol. Biodiesel is a vegetable oil or animal fat-based diesel fuel substitute consisting of long-chain esters as lipid-based biomass. Biodiesel products are commercially available as “B100” and “B5”. Ethanol as ethyl alcohol is another form of biofuel that can be used in petrol engines. It is most commonly derived from sugar-based, lignocellulose biomass

through the fermentation of plant materials including sugar cane molasses, tapioca, paddy straw, cassava and corn. Palm oil biodiesel is often blended with other fuels and used as refined bleached deodorized palm oil (RBDPO), palm stearin, and free fatty acids of palm oil (FFA). From 2005-2010, the Thai Government actively promoted the use of biofuels and this resulted in a 10-fold increase in the production of bioethanol and biodiesel. In 2005, a target was set to reduce diesel consumption by 10% and replace it with biodiesel by the year 2012. In 2007, B5 biodiesel was available at 800 gas stations throughout the country, while by 2018 biodiesel production levels had increased by 142% compared to 2009 **(Table 1)** reflecting the achievement of the Thai Government's energy goal. Consumption targets for ethanol have been set at 4.1 billion liters by 2036, up from 1.18 billion liters in 2015, with biodiesel consumption set to rise to 5.1 billion liters from 1.24 billion liters. Biodiesel production in Thailand is motivated by government directives which are mainly enforced to help palm farmers. There is strict control on imports of palm oil and all palm oil feedstocks used for biodiesel are from domestic sources. Blending of biodiesel by petroleum refineries is also strictly controlled and must adhere to mandatory government requirements. Currently, increased biodiesel production has resulted in 6% blended products compared to diesel consumption **Table 2** shows the feedstock potential for economic crop production of biodiesel (USDA, 2017). The raw material with the greatest potential for biodiesel production is palm oil as this crop provides the highest yield per harvest area.

Table 1 Biodiesel production and consumption in Thailand

Biodiesel (Million Liters)										
Year	**2009**	**2010**	**2011**	**2012**	**2013**	**2014**	**2015**	**2016**	**2017**	**2018**
Production	610	660	630	910	1,080	1,170	1,250	1,240	1,420	1,480
Imports	0	0	0	5	6	12	2	5	5	5
Exports	0	0	0	4	49	4	3	16	20	25
Consumption	609	646	640	890	1,050	1,180	1,243	1,233	1,400	1,470

Table 2 Production and yield of a major oil crops in Thailand (recorded 2009 – 2014)

Oil Crops	Production (1000 ton)				Yield per ha (kg/ha)			
	2009	2012	2013	2014	2009	2012	2013	2014
Oil Palm	8,162	11,353	12,812	13,201	15,996	19,100	20,456	20,144
Soybeans	190	85	70	67	1,588	614	559	575
Coconuts	1,381	1,057	1,057	-	5,804	4,096	3,945	-
Sesame	44	-	-	-	675	-	-	-
Groundnuts	53	-	-	-	1,606	-	-	-
Castor beans	11	-	-	-	863	-	-	-

2.2 Biodiesel from microalgal biomass

Microalgae have the potential for use as a source of renewable energy. Recently, interest in algae has increased as they offer many significant advantages including rapid growth rate and high lipid content as compared to other biofuel crops **(Table 3)** which can be achieved without compromising large areas of arable land (Zhang, Zhao, Cui, Wang, & Liu, 2016). In addition, microalgae capture carbon dioxide efficiently through photosynthesis to produce compounds such as polysaccharides and triacylglycerol (TAG) which are the raw materials for bioethanol and biodiesel and can be used in engines without major modifications (Pulz & Gross, 2004; Vassilev & Vassileva, 2016). By-products such as lubricants, bio-plastics, animal feed, nutraceuticals and pharmaceuticals are also produced from algae (Dahiya, Todd, & McInnis, 2012), while microalgae produce lipids at between 1.5% and 75% (dry weight) utilizing various culture media and procedures (Emmanuel and Nelson, 2016). Lipids accumulate in microalgae cultivated under stress conditions of limited nitrogen supply and/or high salinity (Takagi & Yoshida, 2006), or in association with copper and zinc heavy metals (Einicker-Lamas *et al.*, 2002). Currently there are private companies in Thailand actively producing commercial nutrition food extracted from microalgae. However, there are

no commercial scale facilities for algae derived biodiesel in the country yet. One of the largest problems facing the biofuel business is how to attain high productivity while reducing capital and operating costs (Sawaengsak, Silalertruksa, Bangviwat, & Gheewala, 2014).

Table 3 Comparison of some sources of biodiesel (González-Delgado & Kafarov, 2011)

Raw material	Oil content (%Dry Weight)	Output (L oil/ha year	Land used (m^2 year/kg Biodiesel)	Water Footprint (m^3/ton)	Production Cast (US $/L)	Acid value of oil	Biodiesel Yield (%)
Soybeans	18	636	18	4200	0.40-0.60	0.2	90
Rapeseed	41	974	12	4300	0.99	2.0	87
Sun flower	40	1070	11	6800	0.62	0.1	90
Oil palm	36	5366	2	5000	0.68	6.1	95
Castor	48	1307	9	24700	0.92–1.56	4.6	89
Microalgae *	50	97800	0.1	591 – 3276	3.96–10.56	8.9	60

***** Medium oil content, cultured in photobioreactors

2.3 Biosynthesis of triacylglycerol (TAG)

TAG biosynthesis is a complex process whereby the final TAG assembly reactions may occur via acyl-CoA-dependent and acyl-CoA-independent mechanisms; these are well-defined in oilseed plants, yeasts, and mammals (Coleman & Mashek, 2011; Harwood & Guschina, 2013; Zou *et al*., 1997). In general, triacylglycerols are formed by the sequential acylation of sn-glycerol-3-phosphate (G3P) backbone with three acyl-CoAs catalyzed by a group of enzymes named acyltransferases. This pathway first described by Professor Eugene Kennedy and colleagues in the 1950s is also known as the Kennedy Pathway (Kennedy, 1961). So far, experimental evidence obtained from the studies on enzymes and genes of

TAG biosynthesis in algae is still fragmentary though recent extensive research has provided novel insights and revealed some important and distinctive features of algal oil metabolism (Liu & Benning, 2013). The glycerol-3-phosphate acyltransferase (GPAT, EC 2.3.1.15) initiates this route and transfers acyl moiety from the acyl-CoA pool onto the sn-1 position of G3P, producing lysophosphatidic acid (LPA). Next, the lysophosphatidic acid acyltransferase (LPAAT) inserts the second acyl group into the sn-2 position, converting it into phosphatidic acid (PA) whose dephosphorylation by phosphatidic acid phosphatase (Skopelitis et al.) gives rise to sn-1,2-diacylglycerol **(Figure 2)**. These reactions are common to both membrane lipids and TAG biosynthesis.

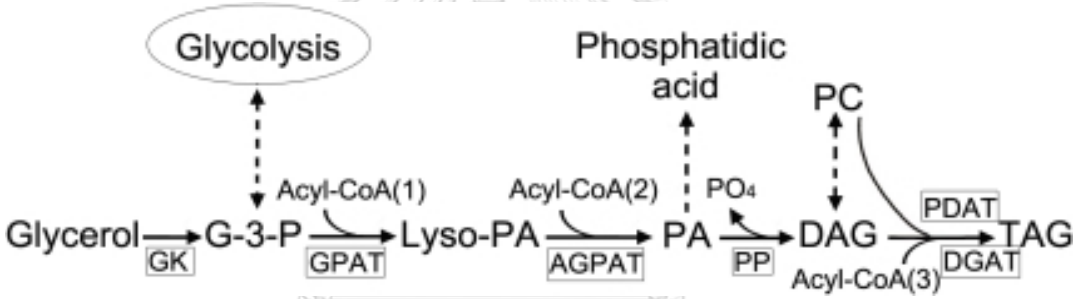

Figure 2 Triacylglycerol biosynthesis pathway. Identified enzymes are shown in boxes and include: GK, glycerol kinase (EC: 2.7.1.30); GPAT, glycerol-3-phosphate acyl transferase (EC: 2.3.1.15); AGPAT, lyso-phosphatidic acid acyl transferase (EC:2.3.1.51); PP, phosphatidate phosphatase (EC: 3.1.3.4); DGAT, diacylglycerol O-acyltransferase (EC: 2.3.1.20) and PDAT, phopholipid: diacyglycerol acyltransferase (EC 2.3.1.158). G-3-P, glycerol-3-phosphate; Lyso-PA, lyso-phosphatidic acid; PA, phosphatidic acid; DAG, diacylglycerol; PC, phosphatidylcholine and TAG, triacylglycerol (Wan *et al*., 2012)

Genes encoding acyltransferases are seen as potential targets for the metabolic engineering of lipid biosynthesis pathways in both higher plants and algae. For example, the heterologous overexpression of GPAT increased seed oil accumulation in oilseed plants (Jain, Coffey, Lai, Kumar, & MacKenzie, 2000). Out of the ten known GPATs in the Arabidopsis genome, GPAT9 (At5g60620) is an ER-localized isoform and is likely involved in the acylation of the sn-1 of the glycerol backbone destined for TAG biosynthesis (Cao, Li, Li, Tobin, & Gimeno, 2006; Gidda, Shockey, Rothstein, Dyer, & Mullen, 2009). The deduced amino acid sequence of AtGPAT9 is most similar to the mammalian GPAT3. Besides four conserved amino acid motifs that are characteristic of GPATs (Lewin, Wang, & Coleman, 1999), both AtGPAT9 and mammalian GPAT3 contain an additional conserved motif in their amino acid sequence distinguishing them from other members of the GPAT family. So far, a number of microalgal acyltransferases, but predominantly DGATs, have been cloned and characterized (Boyle *et al*., 2012; Guihéneuf *et al*., 2011; Xu, Zheng, & Zou, 2009) a few of them have been explored in metabolic engineering approaches to enhance TAG production by heterologous and homologous expression (Iwai, Ikeda, Shimojima, & Ohta, 2014; Niu *et al*., 2013; Sanjaya *et al*., 2013).

2.4 Algal based wastewater treatment

2.4.1 Ammonia in wastewater effluent

Ammonia is the resulting waste product of the aquaculture. All these factors contribute to the high nitrogen residues in aquaculture water. In water ammonia is present in two forms. Unionised ammonia (NH_3), which is more toxic to aquatic life than ionised form (NH_4^+). The proportion of unionised ammonia increases as pH and temperature increase (Ebeling & Timmons, 2012). The sum of the two forms is called total ammonium nitrogen (TAN). The toxicity of NH_3-N to commercially cultured fish at concentrations above 1.5 mg

N L^{-1}. In most cases, the acceptable level of unionized ammonia in aquaculture systems is only 0.025 mg N L^{-1} (Neori *et al*., 2004). However, the toxicity of ammonia to aquatic organisms is reported to differ significantly among species and with life stage. Several previous studies have successfully used algal cultures to remove ammonium from various types of wastewater (Arbib, Ruiz, Álvarez-Díaz, Garrido-Perez, & Perales, 2014). For example, Lim, Chu, and Phang (2010) found that *Chlorella vulgaris* UMACC 001 could reduce NH_4-N concentrations in textile wastewater by 44.4-45.1% (initial concentration = 6.5 mg L^{-1}), while Feng, Li, and Zhang (2011) reported that 97% of NH_4-N was removed by *C. vulgaris* cultivated in artificial wastewater (initial concentration = 20 mg L^{-1}).

2.4.2 Ammonia Assimilation and Recycling

Ammonium is the most preferred form of nitrogen source for microalgae in part because its uptake and utilization by microalgae is most energy-efficient (Perez-Garcia, Escalante, de-Bashan, & Bashan, 2011). In general, ammonium is transported across the membranes by a group of proteins belonging to the Ammonium Transporter family (Azam, Waris, & Nahar). Some ammonium transporters belonging to the AMT family have been found and identified in diatoms and Chlamydomonas (Morris, 1974). The Glutamine Synthetase (GS) and Glutamate Synthase (GOGAT) were reported to catalyze assimilation of ammonium under both autotrophic and heterotrophic culture mode, and at same time producing glutamine, glutamate and 2-oxoglutarate, respectively (Ahmad & Hellebust, 1990). Sometimes ammonium is incorporated into glutamate by the reversible reductive amination of α-ketoglutarate, which is catalyzed by Glutamate Dehydrogenase (GDH) (Inokuchi, Kuma, Miyata, & Okada, 2002). In general, the GS-GOGAT pathway is regarded as the main pathway for ammonium assimilation, while the GDH pathway plays a minor part in the formation of glutamate. However, GDH plays an important role as a catabolic shunt in regulating nitrogen metabolism and mitochondrial function (Lea & Miflin, 2003).

Additionally, the activity of GDH is closely related to conditions of stress. GS has high affinity for ammonia and ability to incorporate ammonia efficiently into amino acids, and is regarded as an important enzyme in photosynthetic microalgae species, even under heterotrophic metabolism (Miflin & Habash, 2002). Nitrogen is distributed to different amino acids after ammonium is incorporated into glutamate via the GS-GOGAT cycle or GDH, much of it through transamination with oxaloacetate by aspartate aminotransferase to yield aspartate (Perez-Garcia *et al*., 2011). The nitrogen assimilation pathways in cyanobacteria show in the **Figure 3**.

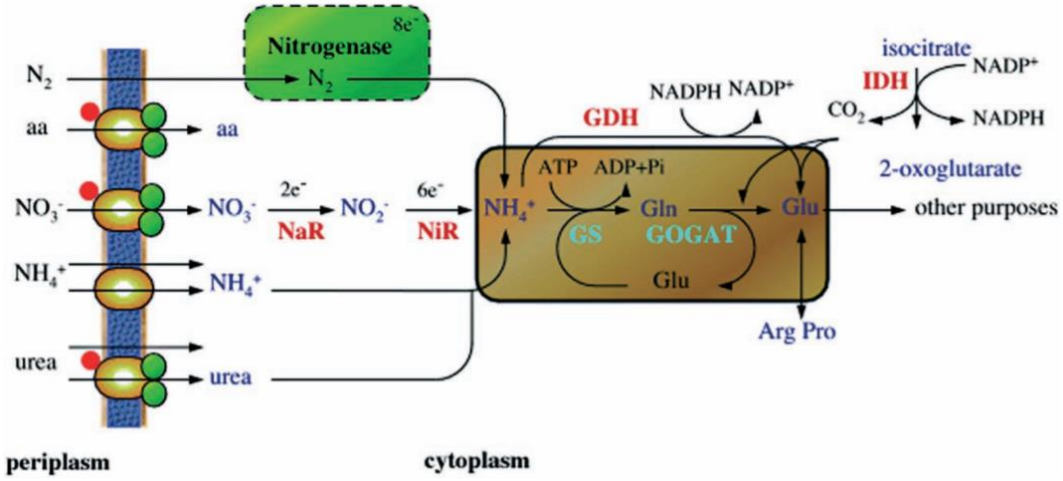

Figure 3 Nitrogen metabolism pathways in cyanobacteria.A continuous line encloses the GS-GOGAT cycle. N_2 fixation by the nitrogenase complex takes place only in some cyanobacterial groups. NaR, nitrate reductase; NiR, nitrite reductase; GS, glutamine synthetase; GOGAT, glutamate synthase; IDH, isocitrate dehydrogenase; GDH, glutamate dehydrogenase (Isabel and Francisco, 2003)

2.5 Response surface methodology (RSM)

2.5.1 Theory and steps for RSM application

Optimizing refers to improving the performance of a system, a process, or a product in order to obtain the maximum benefit from it. The term optimization has been widely used in variety of fields such as chemistry, engineering, materials science and biology as a means of discovering conditions at which to apply a procedure that produces the best possible response (Steinberg & Kenett, 2014). Traditionally, optimization has been carried out by monitoring the influence of one factor at a time on an experimental response. While only one parameter is changed, others are kept at a constant level. This optimization technique is called one-variable-at-a-time. Its major disadvantage is that it does not include the interactive effects among the variables studied. As a consequence, this technique does not depict the complete effects of the parameter on the response. In order to overcome this problem, the optimization of analytical procedures has been carried out by using multivariate statistic techniques. Among the most relevant multivariate techniques used in analytical optimization is response surface methodology (RSM) (Bezerra, Santelli, Oliveira, Villar, & Escaleira, 2008).

RSM was developed by Box and collaborators in the 50s. This term was originated from the graphical perspective generated after fitness of the mathematical model, and its use has been widely adopted in texts on chemometrics (Gilmour, 2006). RSM consists of a group of mathematical and statistical techniques that are based on the fit of empirical models to the experimental data obtained in relation to experimental design. Toward this objective, linear or square polynomial functions are employed to describe the system studied and, consequently, to explore (modeling and displacing) experimental conditions until its optimization (Bezerra *et al*., 2008). The basic idea of this method is to diversify all significant parameters simultaneously over a set of designed experiments and then to combine the results through a mathematical model. Afterwards, this model can be gradually used for optimization,

predictions or interpretation. This leads to improving process performance, reducing the number of variables in the process by taking into account only most significant factors, and also to reducing operation costs and experimental time (Myers, Montgomery, Vining, Borror, & Kowalski, 2004).

The optimization by means of RSM approach could be divided into six stages **(Figure 4)**: (1) selection of independent variables and possible responses, (2) selection of experimental design strategy, (3) execution of experiments and obtaining results, (4) fitting the model equation to experimental data, (5) obtaining response graphs and verification of the model (ANOVA), (6) determination of optimal conditions.

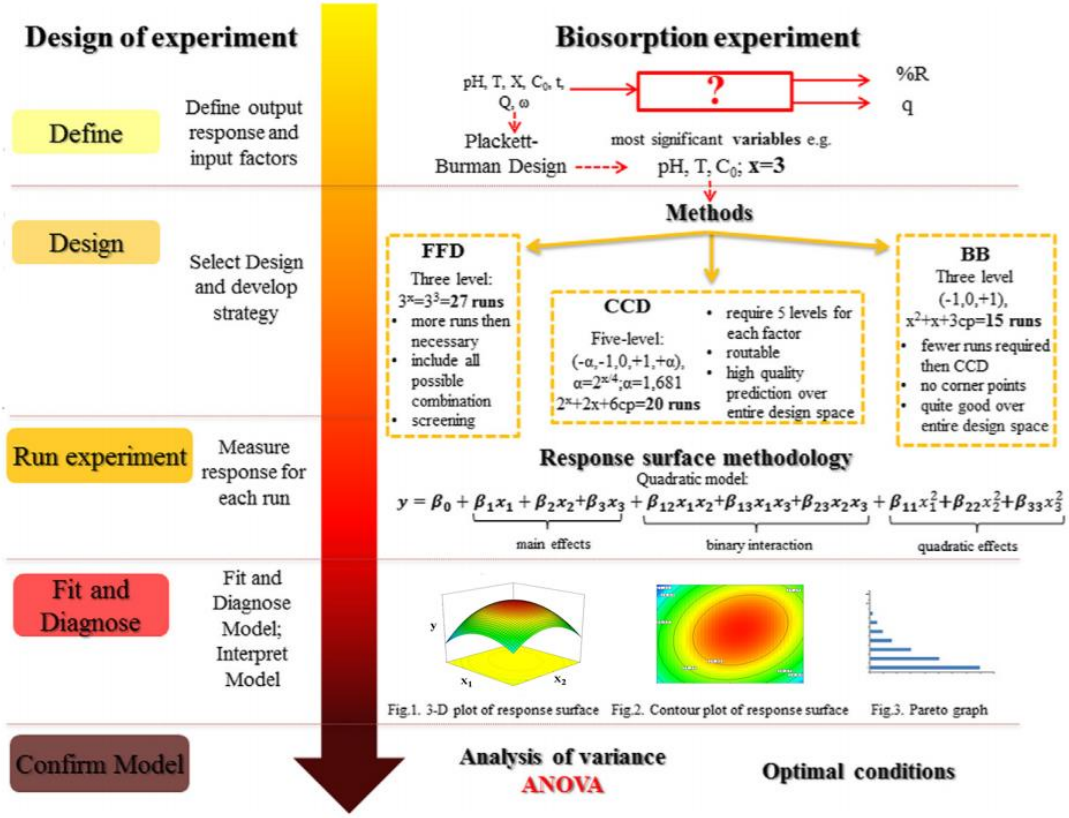

Figure 4 Design of experiment in RSM methodology

(Witek-Krowiak, Chojnacka, Podstawczyk, Dawiec, & Pokomeda, 2014)

2.5.2 Screening of variables

Numerous variables may affect the response of the system studied, and it is practically impossible to identify and control the small contributions from each one. Therefore, it is necessary to select those variables with major effects. Screening designs should be carried out to determine which of the several experimental variables and their interactions present more significant effects. Full or fractional two-level factorial designs may be used for this objective principally because they are efficient and economical (Bezerra *et al.*, 2008)

2.5.3 Selection of experimental design strategy

The next crucial step is the design of an experiment with the selection of the points where the response should be estimated. Several design methods have been applied for biosorption optimization, the most popular being the central composite design (CCD), Box–Behnken design (BB), Doehlert Matrix (D), as well as Plackett– Burman (PB) design, full or fractional factorial designs for optimizations with many variables **(Figure 5)**.

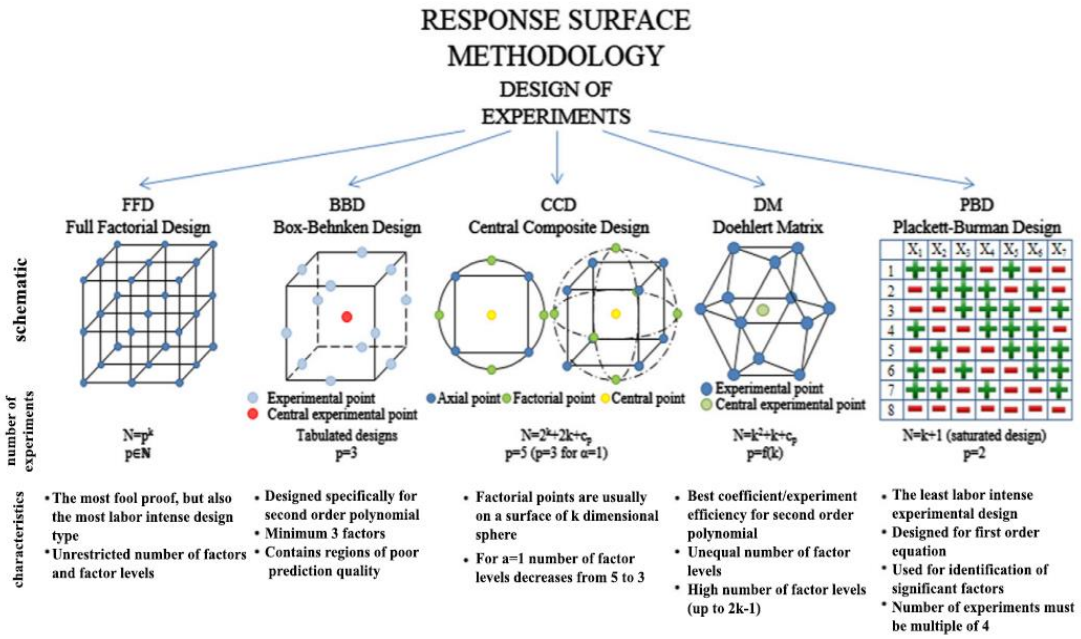

Figure 5 Basic model designs used in RSM

(Witek-Krowiak *et al*., 2014)

2.5.3.1 Central composite design (CCD)

CCD has been widely used statistical method based on the multivariate nonlinear model for the optimization of process variables and also used to determine the operating conditions from the appropriate experiments. It is also useful in studying the interactions of the various parameters affecting the process. CCD yields as much information as the 3n full factorial design (FFD), however this methodology requires a smaller number of experimental runs than FFD. Additionally, CCD provides high quality predictions of linear and quadratic interaction effects of parameters affecting the process. The CCD contains the full factorial or fractional factorial design at two levels (2n), center points (cp), which corresponds to the middle level of the factors, and axial points (2n), which in turn depends on specific properties desired for the design and the number of parameters related (Myers and Montgomery, 2002).

2.5.4 Determination of the optimal conditions

Linear models (represented generically on Eq. (2.1)) allow to specify in which direction the original design should be studied in order to obtain optimal conditions. Nevertheless, if the experimental region cannot be changed, the optimization study should find out the optimal operational conditions by visual inspection (Paulo & Santos, 2017). However, there are many cases where the linear model is not sufficient to represent the experimental data adequately. In this case, more experiments can be performed in addition to those of factorial design and the results can be used to determine a quadratic response surface. For two factors, the model obtained was expressed by Eq. (2.2) ;

$$y = \beta_{\circ} + \sum_{i=\text{i}}^{k} + \beta iXi + \varepsilon \qquad \textbf{(2.1)}$$

where y is the predicted response, X_i are input variables which influence the response variable y, β_0 is the intercept term, β_i is the ith linear coefficient

$$y = \beta_0 + \beta_1 X_1 + \beta_2 X_2 + \beta_{1,2} X_1 X_2 + \beta_{1,1} X_1^2 + \beta_{2,2} X_2^2 \qquad \textbf{(2.2)}$$

where y is the predicted response, β_0 is the intercept term, β_1 and β_2 are linear coefficients, $\beta_{1,2}$ is the logarithmic coefficients, $\beta_{1,1}$ and $\beta_{2,2}$ are quadratic coefficients, X_1 and X_2 were coded independent variables.

2.5.5 The visualization of the predicted model

The model equation predicted using a RSM can be visualized on response surface plots and their related contour plots **(Figure 6)**. The response surface plots are three-dimensional graphs that represent the relationship between factors and the response. Surface response plots are n-dimensional surfaces in the (n+1)-dimensional space. If the system is represented by three or more variables, the graphical representation is only possible if one or more variables are considered constant. The two-dimensional depiction of the response surface plot is the related contour plot. The shape of lines in contour plots may predict the response type. A maximum or minimum response corresponds to ellipses or circles around the plot center.

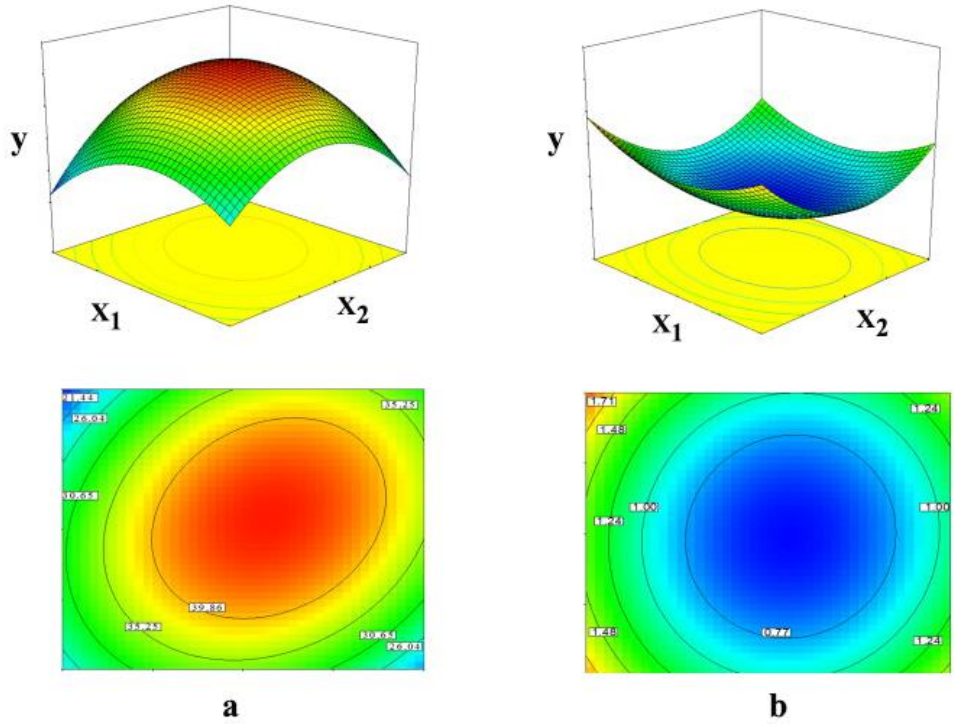

Figure 6 Three-dimensional response surface and the corresponding contour plot

(a) Present the maximum point (b) Present the minimum point

2.6 *Synechococcus* sp.

Genus Synechococcus are some of the most abundant picoplanktonic photoautotrophs in the world's oceans, found either as solitary cells or in small clusters or pairs **(Figure 7)**. *Synechococcus* species also have the ability to adapt to a variety of nutrient concentrations and temperatures (Tsai, Gong, Chung, & Huang, 2018). Recently, *Synechococcus* species have been used as a model for synthetic biology studies, with numerous biotechnological applications including production of biofuels (McNeely, Xu, Bennette, Bryant, & Dismukes, 2010; Ruffing, 2014) and various bioactive compounds. For instance, phycocyanin derived from *Synechococcus* species have radical scavenging and antioxidant potential (Gupta & Sainis, 2010; Sonani *et al*., 2017). Moreover, the genomes of several species of Synechococcus have been fully sequenced, which can provide an understanding of the regulation of gene expression. In this present study, *Synechococcus* sp. (accession number MH393765), marine cyanobacteria originally isolated from Ao Wong Dern, Rayong province, Thailand was investigated.

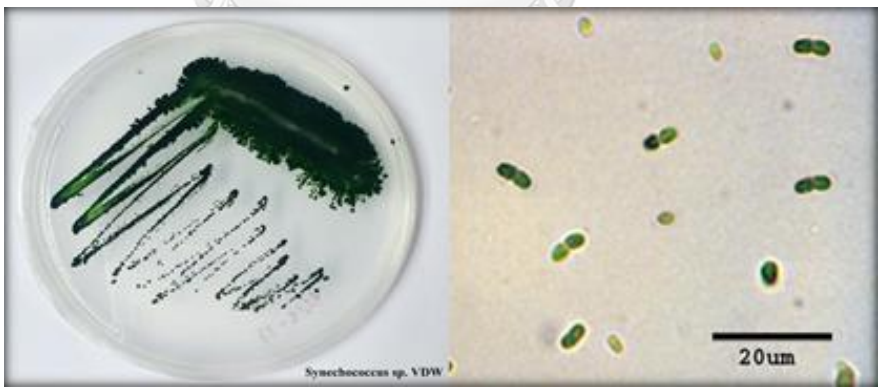

a **b**

Figure 7 *Synechococcus* sp.

(a) Isolated colonies in BG-11 agar plate (b) Morphological under light microscope

CHAPTER III
EXPERIMENTAL

3.1 Algal strain and culture conditions

Synechococcus sp., originally isolated from natural seawater in Thailand, was obtained from Bioenergy Research Unit, King Mongkut's Institute of Technology Ladkrabang, Thailand. This strain was cultured in 250 mL Erlenmeyer flasks containing 100 mL of BG-11 medium supplemented with Turks Island salt solution (pH 7.5) at 30 ± 2°C (Incharoensakdi & Karnchanatat, 2003). Aeration was provided by regular shaking at 150 rpm, and cultures were grown under a fluorescent light irradiance of 30 μmol photon m^{-2} s^{-1} with a 12 h light/12 h dark cycle. Absence of microbial contamination was verified by cultivation on agar medium (E. D. Allen & Gorham, 1981).

3.2 Estimation of biologically relevant ammonium concentrations from shrimp farm effluent

To estimate the concentration of ammonium in standard shrimp farm wastewater, samples of shrimp farm effluent were collected from 5 shrimp farms in Chantaburi Province, one of the largest shrimp farming areas in Thailand. The samples were collected after shrimp harvesting. Sampling procedures and analyses were conducted in accordance with the Standard Methods for the Examination of Water and Wastewater of the American Public Health Association (APHA/AWWA/WEF, 2005). Physicochemical parameters of the wastewater, including biochemical oxygen demand (BOD_5), pH, ammonia (NH_3-N) concentration, total phosphorus (TP) concentration, total Kjeldahl nitrogen (TKN) concentration, and nitrite (NO_2-N) concentration were measured in all samples.

3.3 Effect of ammonium concentration on algal growth and enzyme activity

3.3.1 Experimental set up

To determine the limiting concentration of ammonium on algal growth and enzyme activity, a shake flask growth assay was performed. BG-11 medium without sodium nitrate ($BG\text{-}11_0$) was replaced by ammonium chloride (NH_4Cl) to a final concentration of 10, 20, 30, or 40 mg N L^{-1}, covering the range of concentrations identified in the shrimp farm effluent samples. Three replicate flasks, each containing 100 mL of culture medium, were prepared for each concentration, along with a control (culture medium). These experiments were performed at the same incubation temperature and under the same illumination conditions as for standard culturing. Triplicate flasks for each concentration was collected every 3 days interval for 18 days.

3.3.2 Biomass quantification

The growth of cyanobacterium *Synechococcus* sp was measured by monitoring the optical density (OD) at 730 nm using a microplate spectrophotometer (Multiskan GO, Thermo Scientific, Japan). An aliquot (10 mL) of biomass sample was collected on each sampling day and was vacuum filtered through the filter membrane (0.45 μm). DI water was used to wash sample on the filter for 3 times to wash out chemicals attached on the cell surface. The filter membrane along with biomass was placed in an oven and dried overnight at 90°C. To determine the biomass concentration for a specific OD, A_{730} (Absorbance at 730 nm) was calibrated to result in the cell dry weigh (DW) of *Synechococcus* sp. The relationship between DW and OD_{730} can be described by the following Eq (3.1)

$$\text{Biomass concentration (g L}^{-1}) = 1.8025 \times A_{730} + 0.2177 \quad (R^2 = 0.987) \qquad \textbf{(3.1)}$$

The specific growth rate (μ) was determined from the increase in algal cell density during the exponential growth phase compared with the initial cell density, and calculated using the following Eq (3.2):

$$\mu = \frac{\ln X_t - \ln X_0}{t} \quad \textbf{(3.2)}$$

where X_t is the biomass concentration at time t, X_0 is the cell biomass at the initial logarithmic growth phase, and t is the period between X_0 and X_t.

The remaining culture was harvested by centrifugation at 12,000 ×*g* for 15 min. The cells were washed twice with sterile saline solution (0.85% NaCl) and used for enzyme activity assays (as described in Section 3.3.2). The supernatant was used to measure ammonium concentration (as described in Section 3.5). Samples were measured every 3 days over the 18-day experimental period, including day 0.

3.3.2 Enzyme assays

3.3.2.1 Preparation of cell-free extracts for enzymatic activity assays

The cell pellet was washed twice with 50 mM Tris-HCl buffer (pH 8.0) and then centrifuged at 12,000 × *g* for 15 min at 4°C. The pellet was then resuspended in 3 mL of Tris-HCl buffer and sonicated at 4°C for 3 min (20 s on, 20 s off) at 60 KHz. The sonicated sample was centrifuged at 12,000 × *g* for 15 min at 4°C. The supernatant was transferred into a pre-cooled microfuge tube and used for enzyme assays.

3.3.2.2 Measurement of GS activity

GS activity was measured using the method described by Shapiro and Stadtman (1970). Accordingly, the inorganic phosphate produced during ATP consumption in the biosynthetic reaction (glutamate and ammonium to produce glutamine) was monitored over 15 min and used as a readout of enzyme activity. A negative control assay was performed in the absence of glutamate. One unit of GS activity was defined as the amount of enzyme producing 1 μmol of phosphate per min.

3.3.2.3 Measurement of GOGAT and GDH activity

GOGAT and GDH activities were determined by the colorimetric method of Groat and Vance (1981). One unit of enzyme activity was defined as the amount of enzyme needed to consume 1 μmol of NADH per min.

3.3.2.4 Measurement of protein

The protein concentrations of the extracts were determined according to the method of Bradford (1976), using bovine serum albumin as the standard.

3.4 Effect of ammonium concentration on gene expression

3.4.1 Experimental set up

For experiments addressing the changes in gene expression induced by high ammonium concentrations, algal cells were cultured under the conditions described in Section 3.1. Total cells at mid-logarithmic phase were harvested by centrifugation at 12,000 ×*g* for 15 min, resuspended in 5 mL of sterile saline solution, and then transferred into 100 mL culture medium containing 20 or 40 mg L^{-1} NH_4Cl. Culture medium without NH_4Cl was used as the

control. Samples were then collected at the indicated time points and prepared as described in Section 3.4.2

3.4.2 Preparation of RNA and cDNA synthesis

For RNA extraction from *Synechococcus sp.* , 1 mL of cell culture was sampled at 24, 48, 72, 120, and 168 h after initiation of the light cycle. Cells were collected by centrifugation at 12,000 × *g* for 5 min at 4°C, and then frozen at −80°C until use. Total RNA was extracted using a MasterPure RNA Purification Kit (Epicentre, USA) according to the manufacturer's protocol. RNA was dissolved in 20 µL of TE buffer and then treated with deoxyribonuclease I to eliminate genomic DNA contamination. The total RNA concentration was quantitatively determined using a Nanodrop ND-1000 spectrophotometer (Thermo Fisher Scientific, USA) at 260 nm. Reverse transcription of the total RNA (1 µg) was performed with oligo-dT primers using a Precision nanoScript II Reverse Transcription Kit (PrimerDesign, UK) according to the manufacturer's protocol.

3.4.3 Primer design and qPCR experiments

The nucleotide sequences of genes encoding GS, GOGAT, GDH, and RNase P (housekeeping gene) were retrieved from the GenBank database (https://www.ncbi.nlm.nih.gov/genbank/). All primers used for qPCR assays are showed in **Table 4**. The qPCR was performed using a MyGo Pro Real-time PCR Cycler (IT-IS International Ltd, UK). The 20-µL reaction volumes contained 1 µg of cDNA, 400 nM each primer, and 10 µL of 2× qPCRBIO SyGreen Mix (PCR Biosystem Ltd, UK). Primer specificity was confirmed by the presence of a single band of the expected size on an agarose gel, by a single peak melting curve in the qPCR analysis, and by sequencing of the PCR products. All qPCR protocols started with a 2-min activation step at 95°C, followed by 40 cycles of 10 s at 95°C, 20 s at 60°C, and 30 s at 72°C, and a final melting curve of 55-95°C

for 1 min at each step. The cycle threshold (Ct) was determined in triplicate, and Ct values obtained for each sample were normalized against those of housekeeping gene *rnpB*, encoding ribonuclease P (RNase P). Relative gene expression was calculated using the Ct value, as explained by Livak and Schmittgen (2001), so that the expression was calculated using the following Eq. (3.3) :

$$\text{Relative gene expression} = 2^{-\Delta\Delta Ct} \quad \textbf{(3.3)}$$

where ΔΔCt corresponds to the increase in the threshold cycle of the target gene with respect to the increase in the threshold cycle of the housekeeping gene (*rnp*B, in this study). According to this formula, values of 1 indicate no change; values >1 indicate an increase in gene expression, and values between 0 and 1 indicate a decrease in gene expression**.**

Table 4 Primer sequences and PCR product size of the genes *gln*A, *glt*B, *gdh*A and *rnp*B (housekeeping gene) for qPCR assay used in this study.

Gene	**Product**	**Anti-sense primer (5'-3')**	**product size (bp)**
*gln*A	GS I	Forward: 5'-GTAATGGAGTGCCAGTTGACTGAG-3' Reverse : 5'-CTCAAGGCCGCAGATTATTTGAT-3'	157
*glt*B	NADH-GOGAT	Forward : 5'-AGGAAGGGATTGCGTTCCATA-3' Reverse : 5'-TGCTGATCGTCGTTGTAAGCTG-3'	166
*gdh*A	NADH-GDH	Forward : 5'-AGTCGGAATATGGCTGCTGTTT-3' Reverse : 5'-CATTGTCCGCCGTAATTTGATT-3'	145
*rnp*B	RNase P	Forward : 5'-GGGAGATGCCCTAGCAATCA-3' Reverse : 5'-GGGTTGAATCTGGGGCAGTAG-3'	160

3.5. Measuring the efficiency of ammonium removal

Ammonium concentrations were determined by the indophenol blue colorimetric method according to Koroleff (1983) The supernatants in Section 3.3 were filtered (GF/F grade), and the resulting filtrates were immediately analyzed. After 30 min of incubation at room temperature, the absorbance at 640 nm was used to calculate the ammonium concentrations using a standard curve of NH_4Cl. The ammonium removal efficiency was defined as the percent removal of NH_4^+ from the medium per day, and was calculated using the following Eq. (3.4) :

Removal efficiency (%) = ((conc.start – conc.end)/conc.start)/t) x 100 **(3.4)**

where conc.start is the initial ammonium concentration, conc.end is the final ammonium concentration, and t is the cultivation time.

3.6 Optimization by Response Surface Methodology (RSM)

3.6.1 Experimental set up

The optimal culture conditions to achieve the maximum algal biomass and ammonium removal from synthetic shrimp farm effluent were estimated using the Design-Expert statistical package, version 10.0.6 (Stat-Ease, Inc. Minneapolis, MN, USA). To investigate the interaction between the parameters, a central composite design (CCD) was applied. Three parameters, initial solution pH (x_1), inoculums size (x_2), and initial ammonium concentration (x_3) were studied. Therefore, the full design matrix consists of eight factorial points, six axial points and three replicates at the center points, resulting in a total of 17 experiments as shown in Eq. (3.5):

$$N = 2^n + 2n + n_c = 2^3 + 2(3) + 3 = 17 \quad \textbf{(3.5)}$$

where N is the number of experiments, and n is the number of factors.

Seventeen experiments were conducted in 100 mL Erlenmeyer flasks containing culture medium of different pH, inoculum size and initial ammonium chloride (NH_4Cl) concentration as shown in **Table 5**. The percentage biomass production and ammonium removal were considered as dependent variable (response).

Table 5 Level and range of variables in the experiments

Variables	Code levels				
	-1.68	**-1**	**0**	**1**	**1.68**
X_1 : pH	6.66	7.0	7.5	8.0	8.34
X_2 : inoculums size (OD_{730})	0.06	0.1	0.15	0.2	0.23
X_3 : ammonium concentration (mg N L^{-1})	4.96	7.0	10.0	13.0	15.04

The design matrix contained a 2^3 factorial design augmented by six axial points coded ±α and three central points (all factors = zero). The value of α was calculated by Eq. (3.6):

$$\alpha = 2^{n/4} \quad \textbf{(3.6)}$$

where n is the number of factors in the design. Therefore, α is equal to $2^{3/4} = 1.682$ according to Eq. (3.6). The range and levels of all factors in coded and real values were calculated by Eq. (3.7):

$$x_i = \frac{X_i - X_{ic}}{\Delta X_i} \quad \textbf{(3.7)}$$

where x_i is the coded value of the *i*th test variable; X_i is the uncoded value of the *i*th test variable, X_{ic} is value of X_i at the center point of the studied area, and ΔX_i is the step size.

The quadratic polynomial equation was fitted to correlate the relationship between independent variables and responses as shown in Eq. (3.8):

$$Y = \beta_0 + \sum_{i=1}^{3} \beta_i x_i + \sum_{i=1}^{3} \beta_{ii} {x_i}^2 + \sum_{i,j=1}^{3} \beta_{ij} x_i x_j \quad \textbf{(3.8)}$$

where Y is the predicted response, x_i and x_j input variables, β_0 intercept, β_i linear coefficient, β_{ii} quadratic coefficients and β_{ij} interaction coefficients.

3.6.2. Biomass production

After seven days of cultivation, 10 mL aliquots of samples from each experimental run were collected and the optical density (OD) was measured at 730 nm using a microplate spectrophotometer (Multiskan GO, Thermo Scientific, Japan). The biomass concentration for a specific OD, A_{730} was calibrated to result in the cell dry weigh (DW) of *Synechococcus* sp. The relationship between DW and OD730 can be described by the following Eq (3.1). The biomass production in term of percentage increase in cell density was calculated using Eq. (3.9):

$$\text{Biomass production (\%)} = \frac{S_t - S_0}{S_0} \text{x } 100 \quad \textbf{(3.9)}$$

where S_0 is the biomass concentration at day 0, S_t is the biomass concentration at day 7.

3.6.3. Efficiency of ammonium removal

Ammonium concentrations were determined by the indophenol blue colorimetric method according to Koroleff as described in Section 3.4.2. The ammonium removal was defined as the percentage of NH_4^+-N removal from the medium at day 7, and was calculated using Eq. (3.10):

$$\text{Ammonium removal } (\%) = \frac{C_0 - C_t}{C_0} \text{ x } 100 \qquad \textbf{(3.10)}$$

where C_0 is the initial ammonium concentration (mg L^{-1}) and C_t is the final ammonium concentration (mg N L^{-1}).

3.7. Changes of fatty acid profiles and GPAT gene expression under optimum condition

3.7.1 Fatty acid characterization

The fatty acid components of *Synechococcus sp.* under normal and optimal condition were analyzed by gas chromatography-mass spectrometry (GC-MS) based on the method described by Lepage and Roy (1986). Briefly, 7 day-old microalgae cultures were collected, after which 3 g of sample were transferred into screw cap tubes. Next, 12.0 mL of dicloromethane:methanol (2:1 v/v) were added and sample were allowed to stand for 1 h, during which time they were vortexed every 15 min. The samples were subsequently filtrated through Whatman no.1 filter paper, after which 0.1 M KCl was added. The samples were subsequently vortexed briefly, then centrifuged at 2,000 × g for 10 min and the upper phase was discarded. Samples were then methylated by adding 1 mL of 0.5 mol mL^{-1} NaOH-methanol to 200 µL of the product from the previous step and heating the tubes for 15 min at 100°C. Next, samples were allowed to cool to room temperature, after which 500.0 µL of

hexane and 5 mL of saturated NaCl solution were added. The samples were then vortexed briefly and centrifuged at 2,000 × g for 5 min, after which the organic (upper) phase was transferred to a fresh tube. GC-MS analyses were subsequently performed using Trace-GC Ultra (Thermo Scientific, *Italy*) equipped with 60 m × 0.25 mm TR-FAME capillary column (Thermo Scientific, USA) connected to a PolarisQ mass spectrometer (Thermo Scientific, USA). The fatty acid profiles were identified by comparison with commercial standards and the area normalization method was employed to quantify the relative percentage of individual fatty acids. All samples were analyzed in duplicates.

3.7.2 Degree of saturation (DU)

Degree of saturation parameter was determined by Eq. (3.11). (Ramos *et al*., 2009)

DU = (mono-unsaturated, wt. %) + 2 (poly-unsaturated, wt. %) **(3.11)**

3.7.3 Gene expression assay

Algal cells were cultured under the conditions described in Section 3.1. Total cells at mid-logarithmic phase were harvested by centrifugation at 12,000 ×*g* for 15 min, resuspended in 5 mL of sterile saline solution, and then transferred into 100 mL of optimum medium from Section 3.6. Normal medium was used as the control. Samples were then collected at 48 and 72 h, respectively.

Primer specific for the gene encoding GPAT were designed using the primer BLAST tool at the NCBI website (http://www.ncbi.nlm.nih.gov/tools/primer-blast/). All primers used for qPCR are shown in **Table 6**. The qPCR experiments were described in Section 3.4.2-3.4.3).

Table 6 Primer sets used for quantitative PCR

Gene	Primer	Sequence	Product size (bp)
GPAT	Forward primer	GCCGTGGCTATTTAACATCGA	133
GPAT	Reverse primer	GCGAATTGGTGGACAGACCC	
*rnp*B	Forward primer	ACCTCTCGATG(C/T)TGCTGGTG	140
*rnp*B	Reverse primer	TTGCTGGGTAACGCCCAGTG	

3.8 Statistical analysis

Three experimental replicates were carried out for each assay, with at least three analytical replicates per sampling point. All calculations were performed using Statistical Package for Social Sciences (SPSS) version 15.0 (SPSS, Inc., USA). Univariate analysis of variance and post-hoc and Duncan tests were used for analysis. All capacity measures are given as means ± standard error over the duration of the examined using analysis of variance (ANOVA) with Scheffe post-hoc testing. Mean differences were determined to be significant at $p<0.05$.

The Design Expert statistical package was used for regression analysis of variance (ANOVA). All experiments were conducted in triplicate, and the average values were recorded as the response. The quality of fit of the polynomial model equation was expressed by the coefficient of determination (R^2) and the adjusted R^2 (R^2_{adj}), and its statistical significance was assessed with a P-value. 'Statistica 7.0' was used for the graphical. The optimum values of the selected variables were obtained by analyzing the response surface and contour plots and also by analyzing the quadratic polynomial equation (Ramesh, Muthuvelayudham, Rajesh Kannan, & Viruthagiri, 2013).

CHAPTER IV
RESULTS AND DISCUSSION

4.1. Analysis of shrimp farm effluent

As shown in **Table 7**, pH levels and concentrations of TP and NO_2-N were not higher than standard values for effluent. In contrast, concentrations of BOD_5, NH_3-N, and TKN exceeded the permitted limits by 3, 15, and 4 times, respectively. To cover the range of ammonium concentrations identified in the shrimp farm effluent samples, NH_4Cl was used at 10.0–40.0 mg N L^{-1} in this study.

Table 7 Characteristics of the samples of shrimp farm effluent at Chantaburi province

Parameter	Unit	Standard *	Mean (±SD)	Analytical Method
pH		6.5 – 9.0	7.12±0.68	pH meter
Biochemical Oxygen Demand (BOD_5)	mgL^{-1}	≤ 20	54.94±17.36	Standard method #5210 B
Ammonia nitrogen (NH_3-N)	mgL^{-1}	≤ 1.1	16.50±3.33	HACH method #8155
Total Phosphorus (TP)	mgL^{-1}	≤ 0.4	0.44±0.12	HACH method #8190
Total Kjeldahl Nitrogen (TKN)	mgL^{-1}	≤ 0.4	14.86±2.85	HACH method #10242
Nitrite (NO_2-N)	mgL^{-1}	≤ 0.28	0.22±0.07	HACH method #8507

* Effluent qualities Standard for coastal aquaculture (Manual for Water and Wastewater Examination of Environmental Engineering Association of Thailand)

4.2. Growth response to ammonium

The growth curves for *Synechococcus* sp. grown in the presence of different initial ammonium concentrations (10, 20, 30, or 40 mg L^{-1} NH_4^+-N) are shown in **Figure 8**. The cell density decreased slightly with an increase in the ammonium concentration. The highest specific growth rates for each of the concentrations of ammonium were 0.11, 0.05, 0.03, 0.03, and 0.04 d^{-1}, respectively. These results indicate that the growth of *Synechococcus* sp. was promoted by supplementation of the growth medium with NH_4^+ in the range of 1.0–10.0 mg L^{-1}, but was obviously inhibited when the NH_4^+ concentration increased to 20.0 mg L^{-1} or higher. Supporting this finding, S. Allen and Smith (1986) suggested that high concentrations of ammonium may inhibit growth of photosynthetic organisms. One explanation is that the excretion of protons, produced during ammonium assimilation, into organic matter may increase the acidity, resulting in damage to the organisms.

Biomass concentration (g L^{-1})

Time (days)

Figure 8 Effect of ammonium concentrations on growth of *Synechococcus* sp. for 18 days. (○) BG-11 (control), (●) 10.0 mg N L^{-1}, (△) 20.0 mg N L^{-1}, (▲) 30.0 mg N L^{-1}, and (□) 40.0 mg N L^{-1}. Data shown are means (along with the standard deviations, SE) of at least three independent experiments

4.3. Effect of ammonium concentration on the activity of key ammonium assimilation enzymes

The activity of three key ammonium assimilation enzymes was measured, and results are shown in **Figure 9** (a-c). GS and GOGAT activities were highest in mid exponential phase cells (day 12 of cultivation) in the media containing 10.0 mg L^{-1} NH_4-N, then decreased to very low levels by stationary phase. This may indicate that all the available ammonium was used by the cells under these conditions. Meanwhile, enzyme activity was suppressed when the ammonium concentrations were higher than 20.0 mg L^{-1}. In contrast, the observed GDH activity was lowest in cells grown under the low-ammonium concentration conditions (10.0 mg L^{-1} NH_4-N). Mérida, Candau, and Florencio (1991) reported that addition of 0.25 mM NH_4C1 caused a rapid decrease in GS activity in *Synechocystis* sp. PCC 6803. Inactivation of GS has been reported in the cyanobacterium *Synechocystis* sp. PCC 6803, with the dramatic effect produced by L-methionine-DL-sulphoximine, a specific inhibitor of GS. In addition, Chávez, Lucena, Reyes, Florencio, and Candau (1999) demonstrated that a mutant strain of *Synechocystis* sp. PCC 6803 lacking GDH had no change in its rate of ammonium assimilation. Therefore, the major metabolic route for ammonium assimilation in cyanobacteria is the GS-GOGAT pathway. Similar to enterobacteria, GDH plays an auxiliary role in *Synechococcus*, operating as the only assimilation pathway in media containing high concentrations of ammonium (Brenchley & Magasanik, 1974). Moreover, Skopelitis *et al*. (2006) reported that under stress conditions, when the GS-GOGAT system was not fully operating, an increase in GDH activity may counteract the accumulating toxic amounts of NH_4^+, and provide glutamate for the biosynthesis of protective compounds such as proline.

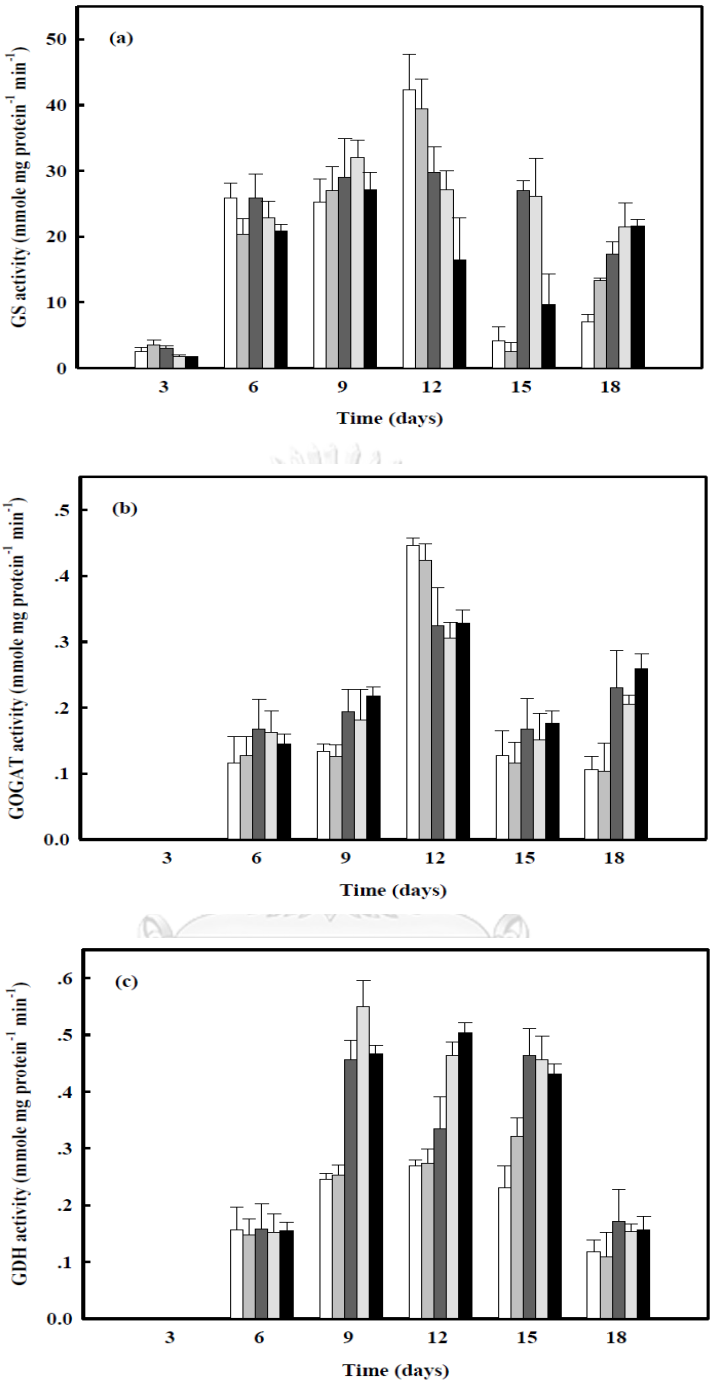

Figure 9 The effect of ammonium concentrations on GS, GOGAT, and GDH activities as present on a-c respectively, in the presence of (white) control, (grey) 10.0 mg N L^{-1}, (dark grey) 20.0 mg N L^{-1}, (light grey) 30.0 mg N L^{-1}, and (dark) 40.0 mg N L^{-1}. Data shown are means (along with the standard deviations, SE) of at least three independent experiments

4.4. Effect of ammonium concentration on gene expression

Differences in relative gene expression levels in response to ammonium-rich conditions (20.0 and 40.0 mg L^{-1}) compared with the control (1.0 mg L^{-1}) were determined by qPCR. As shown in **Figure 10** (a-c), *glnA*, *gltB*, and *gdhA* were similarly expressed under ammonium-rich conditions. After 24 h, the relative expression of these genes was down-regulated compared with the control. The maximum relative expression of *glnA* (~2-fold increase) was observed in cells incubated in BG-11_0 containing 40 mg L^{-1} NH_4-N at 168 h post-inoculation. The expression of *gltB* in BG-11_0 containing 20.0 mg L^{-1} NH_4-N was lower than that under control conditions, while at 40.0 mg N L^{-1} NH_4Cl, cells showed slightly higher expression of *gltB* **(Figure 9b)**. Interestingly, under ammonium rich conditions, the expression of *gdhA* **(Figure 9c)** was greatly increased compared with the control. The two highest levels of *gdhA* expression (2.1 and 1.9-fold increases) were observed in cells incubated in media containing 20 and 40 mg L^{-1} NH_4-N at 168 and 48 h post-inoculation, respectively. These results suggest that *gdhA* was induced by nitrogen-rich conditions, while *glnA* and *gltB* were repressed. Clearly, the changes in the transcriptional levels of *glnA*, *gltB*, and *gdhA* corresponded to the observed levels of GS, GOGAT, and GDH activity, leading to the conclusion that these enzymes are similarly regulated under the same ammonium conditions **(Figure 11).**

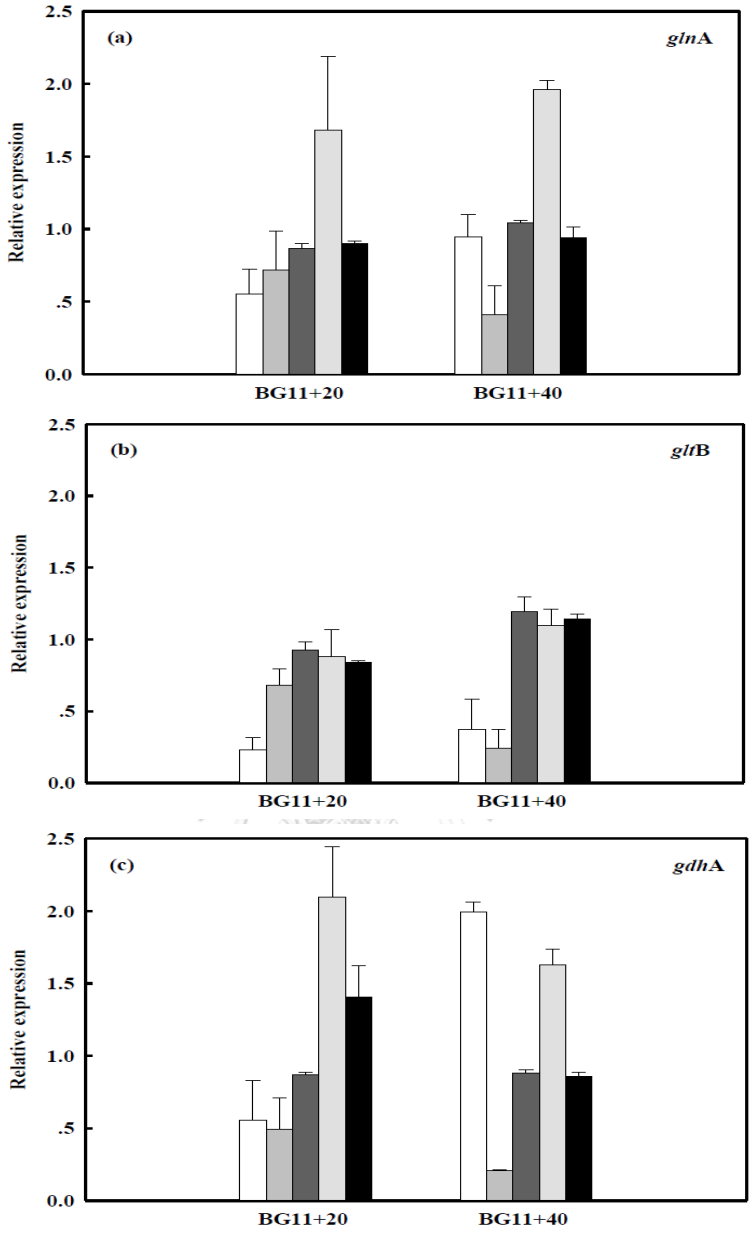

Figure 10 Effect of ammonium concentration on the gene expression of *Synechococcus* sp. (a) *gln*A gene : (b) *glt*B gene : (c) *gdh*A gene, as monitorized by qPCR analysis. After 14 days of cultivation in culture medium, *Synechococcus* sp. was subjected to BG-11_1 medium treated with high concentration (20 and 40 mg N L^{-1}) of NH_4Cl. The samples were taken at; (white) 24 h, (grey) 48 h, (dark grey) 72 h, (light grey) 120 h, and (dark) 168 h. Data are means ± S.E. (n = 3)

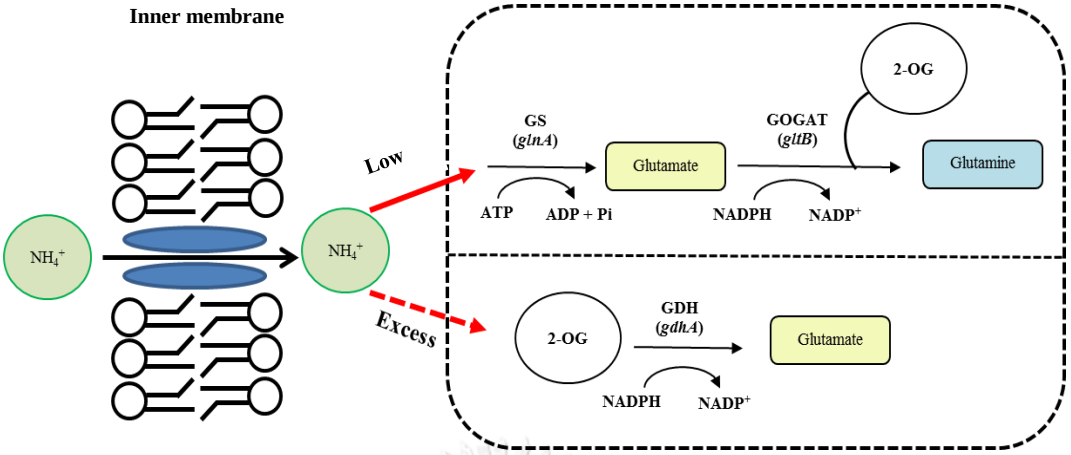

Figure 11 The schematic model of the ammonium assimilation network of *Synechococcus* sp. Arrows denote the direction of the reactions. GS, GOGAT and GDH denote the enzymes catalyzing the reactions. For GDH, one mole of 2-oxoglutarate and NH_4^+ are converted to one mole Glutamate. GS-GOGAT cycle, one ATP is needed to form one Glutamate. Under low ammonium, glutamate is made primarily through GS-GOGAT pathway. The GDH pathway is used in glutamate synthesis when the cell is limited for energy but ammonium is present in excess

4.5. Effect of ammonium concentration on ammonium removal efficiency

To evaluate the ammonium removal efficiency of *Synechococcus sp.* , cells were exposed to different concentrations of ammonium for 6 days prior to ammonium concentration analysis. The ammonium removal efficiencies ranged from 16.5% in 10.0 mg L^{-1} NH_4-N medium to 5.15% in medium supplemented with 40.0 mg L^{-1} NH_4-N **(Table 8)**. Total ammonium removal reached a maximum level of 98% in the treatment containing 10.0 mg L^{-1} NH_4-N, and there was no significant difference between this treatment and the control. However, the ammonium removal efficiency decreased after 6 days of cultivation (data not showed). These results revealed that ammonium concentrations greater than 20.0 mg L^{-1} could decrease the ammonium removal efficiency by this strain. Borowitzka (1998) also reported that ammonium concentrations greater than 20.0 mg L^{-1} were not recommended because of ammonium toxicity, and moreover, photosynthesis in marine diatoms is inhibited

under high ammonium conditions. In general, average ammonium concentrations in aquaculture wastewater range from 0.5–20.0 mg L^{-1} (Pham, Schideman, Scott, Rajagopalan, & Plewa, 2013).

Table 8 Initial concentration, final concentration and bioremediation efficiencies of ammonium by *Synechococcus* sp. after exposure to four different ammonium concentrations for 6 days.

Initial Concentration Of NH_4Cl (mg N L^{-1})	**% Removal**	**Removal efficiency (% NH_4-N d^{-1})**
10	98.03[a]	16.45[a]
20	58.49[b]	9.75[b]
30	53.00[c]	8.83[c]
40	30.90[d]	5.15[d]

Different letters within the same column represent statistically different values ($p < 0.05$). Values represents means ± SE, n = 3.

4.6. Optimization by response surface methodology

The maximum efficiency of ammonium removal and biomass production by *Synechococcus* sp. were investigated under different operating conditions; namely, initial pH 6.66–8.34, inoculum size 0.06–0.23 and initial ammonium concentration 4.96–15.04 mg N L^{-1}. The design matrixes of the variables determined by CCD along with the predicted and experimental values of responses are given in **Table 9**. The results were analyzed by analysis of variance (ANOVA) as shown in **Table 10**.

The coefficient and *p*-values of all the variables of linear (x_1, x_2, x_3), quadratic (x_1^2 x_2^2, x_3^2) and interactions (x_1x_2, x_1x_3, x_2x_3) terms were determined according to ANOVA. Larger *f*-value and smaller *p*-value represent a high significance of the corresponding coefficient.

P-values < 0.05 were considered to indicate significance (Dinarvand *et al*., 2013). The results of ammonium removal showed that x_1, x_3, x_1x_3, x_2x_3, x_1^2, x_2^2 and x_3^2 were significant terms; therefore, they were selected as the effective terms while other model terms were deleted. In addition, the model *f*-value of 133.44 for Y_1 (ammonium removal) and the *p*-value (< 0.0001) for the overall model showed that the overall model is significant. The *p*-value of lack of fit was 0.0589 (non-significant), indicating that the model fit the experimental data well and the independent variables have considerable effects on the response. Analysis of variance of the biomass production showed that x_3, x_1^2, x_2^2 and x_3^2 were significant ($p < 0.05$). Moreover, the coefficient of determination (R^2) was calculated as 0.9942 for ammonium removal and 0.9609 for biomass production, indicating that the regression model represented 96-99% of the experimental results, while about 1-4% of the variability in the response was not explained by this model (Niazi, Khorshidi, & Ghaemmaghami, 2015). Additionally, the ANOVA table of the fitted model **(Table 10)** indicated that the regression was significant ($p = 0.0004$), while the lack of fit was not significant ($p > 0.05$). These results suggest that the

design model adequately fits the experimental data. As a result, the following regression models were showed in Eq. (4.1) and (4.2):

$$Y_1 = 98.1 - 5.69x_1 - 22.46x_3 + 6.5x_1x_3 - 4.25x_2x_3 - 20.86x_1^2 - 5.83x_2^2 - 16.79x_3^2 \quad \textbf{(4.1)}$$

$$Y_2 = 78.33 - 22.13\,x_3 - 11.75\,x_1^2 - 5.41\,x_2^2 - 10.96x_3^2 \quad \textbf{(4.2)}$$

where Y_1 and Y_2 are the predicted response of ammonium removal and biomass production; x_1 is the pH; x_2 is the inoculum size; x_3 is the ammonium concentration.

Table 9 Responses for biomass production and ammonium removal

Run	pH	Inoculum size (OD_{730})	NH_4Cl conc. (mg N L^{-1})	Ammonium removal (%)		Biomass production (%)	
				Observed	Predicted	Observed	Predicted
1	0	0	0	99.07	98.10	80.20	78.33
2	1	1	1	33.99	28.82	24.14	28.08
3	1	-1	1	30.70	37.32	20.16	28.08
4	1	1	-1	70.15	69.04	54.00	72.34
5	-1	-1	-1	83.33	85.12	71.23	72.34
6	0	0	0	98.80	98.10	76.16	78.33
7	0	1.68	0	87.34	81.61	70.14	63.03
8	0	-1.68	0	78.21	81.61	60.72	63.03
9	-1	1	-1	95.12	93.62	82.75	72.34
10	-1.68	0	0	50.33	48.67	49.00	45.10
11	1.68	0	0	30.87	29.53	45.87	45.10
12	-1	-1	1	38.67	35.50	33.00	28.08
13	0	0	-1.68	88.56	88.38	87.33	84.55
14	0	0	1.68	15.08	12.84	12.00	10.11
15	0	0	0	97.13	98.10	78.30	78.33
16	1	-1	-1	60.44	60.54	74.11	72.34
17	-1	1	1	22.13	27.00	29.22	28.08

Table 10 Analysis of variance (ANOVA) of ammonium removal and biomass production by response surface quadratic model

Source	df	Ammonium removal (%) (Y_1)				Biomass production (%) (Y_2)			
		Sum of square	Mean square	*f*-value	*p*-value	Sum of square	Mean square	*f*-value	*p*-value
Model	9	14299.52	1588.84	133.44	< 0.0001 [a]	8338.03	1023.03	19.14	0.0004 [a]
x_1	1	441.42	441.42	37.07	0.0005 [a]	69.8	176.2	3.3	0.1123
x_2	1	46.24	46.24	3.88	0.0894	11.71	3.81	0.071	0.7971
x_3	1	6891.23	6891.23	578.77	< 0.0001 [a]	5909.43	6689.98	125.15	< 0.0001 [a]
x_1x_2	1	40.47	40.47	3.4	0.1078	221.03	71.22	1.33	0.2863
x_1x_3	1	337.91	337.91	28.38	0.0010 [a]	85.35	7.9	0.15	0.7121
x_2x_3	1	144.56	144.56	12.14	0.0102 [a]	11.02	9.66	0.18	0.6836
x_1^2	1	4903.45	4903.45	411.83	< 0.0001 [a]	1409.03	1555.42	29.1	0.001 [a]
x_2^2	1	383.12	383.12	32.18	0.0008 [a]	283.99	329.8	6.17	0.042 [a]
x_3^2	1	3177.93	3177.93	266.91	< 0.0001 [a]	1217.16	1353.48	25.32	0.0015 [a]
Residual	7	83.35	11.91			225.72	53.45		
Lack of fit	5	81.35	16.27	16.27	0.0589	217.72	73.07	16.56	0.0579
Pure error	2	2	1			8	4.41		
Total	16	14382.86				8563.75			
R^2		0.9942				0.9609			
R^2_{adj}		0.9868				0.9107			

[a] Model terms are significant.

4.7. Graphical description of the model equation

The 3-D response surfaces and contour plots developed using Eq. (4.1) for ammonium removal and Eq. (4.2) for biomass production are shown in **Figure 11**. The optimization of pH, inoculum size and ammonium concentration for the maximum ammonium removal and biomass production was conducted in the range of experimental runs using the Design Expert software. The optimal pH, inoculum size, and ammonium concentration were found to be 7.4, 0.15 (OD_{730}), and 10.62 mg N L^{-1}, respectively, which yielded an optimal algal growth of about 75.5% (0.11 g L^{-1} of dry cell weight) and an average ammonium removal of 90%. These results agreed well with the predicted value of algal growth and ammonium removal of 73.5% and 92.9%, respectively. The combined effects of pH and ammonium concentration was found to be the dominant factor influencing ammonium removal, while ammonium concentration had a significant effect on algal growth. These findings are consistent with those of Chen *et al*. (2015) who found that the specific growth rate *of Chlorella pyrenoidosa* decreased by approximately 12.7%–23.1% at a pH of 8.5–9.0, while pH variations between 6.5 and 8.5 had no significant influence on growth. Conversely, they found that the specific growth rate decreased by more than 50% and 80% when the ammonia concentration increased to 30–40 and 50–60 mg L^{-1}, respectively. In general, there are two forms of ammonia, ionized (NH_4^+) and un-ionized (NH_3). As pH increases, the toxicity of ammonia increases because the relative proportion of unionized ammonia, which is known to be toxic to several photosynthetic organisms, increases. However, Caicedo, Van der Steen, Arce, and Gijzen (2000) found that both ammonia forms caused growth inhibition via inhibition of photosynthesis.

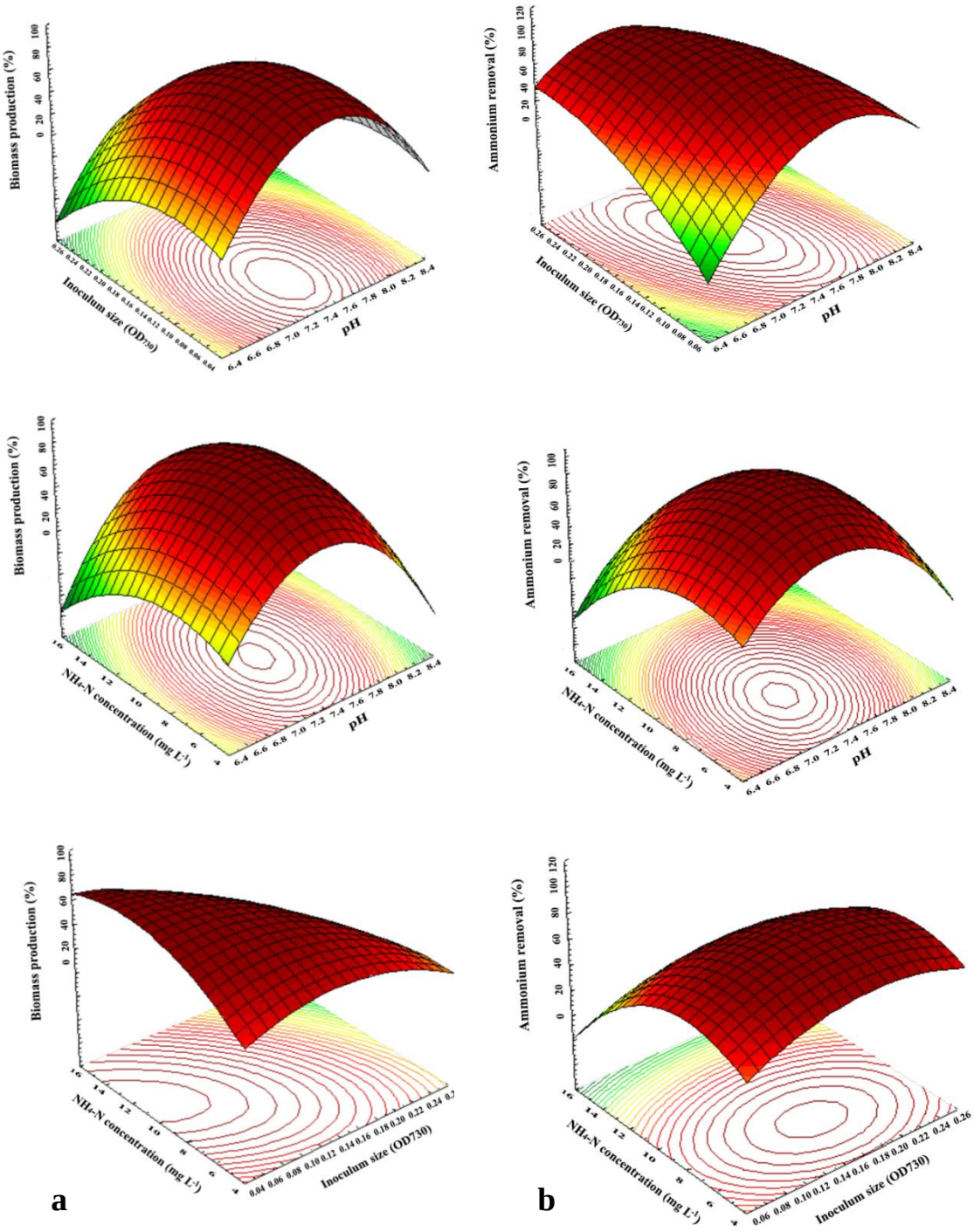

Figure 12 Response surface and contour plot showing effects and interaction of inoculum size and pH, ammonium concentration and pH, and ammonium concentration and inoculum size on (a) ammonium removal, % and (b) biomass production, %.

An additional experiment was then performed to confirm the optimum results. As showed, the maximum ammonium removal and biomass production were 93.27 and 77.10, respectively. The laboratory experiment agrees well with the predicted response value. The result from **Table 11** shows that there is a good agreement between the predictive and experimental results at the optimum levels, giving a high validity of the model (% error less than 5).

Table 11 Optimization results for independent variables and responses in predicted and experimental values

Optimum condition			**Ammonium removal (%)**			**Biomass production (%)**		
X_1	X_2	X_3	predicted	Experimental	Error (%)	predicted	Experimental	Error (%)
7.4	0.15	10.62	90.0	93.27 ±0.21	1.85	75.50	77.10 ±0.53	2.25

X_1 = pH X_2 = inoculum size X_3 = NH_4 concentration

4.8. Fatty Acid Composition

The fatty acid composition of *Synechococcus* sp. was evaluated in the early stationary growth phase by GC-MS analysis. Total fatty acid profiles indicated seven fatty acids in normal condition, while six were found in cells cultivated under optimal conditions. Under both conditions, dominant long-chain fatty acids consisted of 16 and 18 carbon atoms with four major constituents as palmitic acid (C16:0), linoleic acid (C18:2 n6 cis), palmitoleic acid (C16:1) and oleic acid (C18:1 n9 cis) accounting for more than 80% of the total **(Table 12)**. Percentages of saturated fatty acids and monounsaturated fatty acids decreased (≤5 wt.%)

with increasing polyunsaturated fatty acids (~14 wt.%) compared to normal condition. Previous studies have shown that various stresses such as nitrogen concentration, pH, salinity and light are commonly used to induce polyunsaturated fatty acid (PUFA). PUFA play a prominent role as the osmo-protecting molecules may help microalgal cells confront environtment stresses, and these mechanisms, in turn, stimulate the biosynthesis of lipids as energy-rich storages in microalgal cells (Chen et al., 2015; Wang et al., 2016). Although giving slightly lower saturated fatty acids when compared to the control, however, palmitic acid content showed similar to fatty acid in palm oil **(Table 13)**. Palmitic acid has a higher cetane number (McNeely et al.) as the most important indicator of diesel in terms of ignition quality with a higher value indicating better grade (Azam *et al*., 2005). Degree of unsaturation (DU) indicates the number of double bonds present in the fatty acid chain with a high number of double bonds representing a high degree of unsaturation. Ramos, Fernández, Casas, Rodríguez, and Pérez (2009) suggested that higher unsaturation in oil was associated with higher CN and iodine value. In comparison with other feedstocks, the DU value of *Synechococcus* sp. was similar to olive oil but higher than the commercial biodiesel feedstock palm oil. Ramos *et al*. (2009) reported that the CN of olive oil presented near to palm oil at 57 and 61 respectively, while soybean and sunflower oil presented CN values lower than the European Standard (minimum CN of 51). As a result, oils with DU higher than 137 do not meet European Standards for cetane number and iodine value. Low CN were associated with more highly unsaturated components such as esters of linoleic (C18:2) and linolenic (C18:3) acids (Knothe, Matheaus, & Ryan III, 2003). Li, Yang, Zhou, and Yu (2018) discovered that higher DU values resulted in increased nitrogen oxide (NO_x) emissions. High levels of unsaturation adversely affect engine performance and exhaust gases with the degree of biodiesel unsaturation resulting in small variations of oxygen content, heating value and viscosity (Altun, 2014) . Results indicated that biodiesel quality from

Synechococcus sp. in terms of CN and iodine values almost attained the European Standards criteria; hence, this strain shows promise for use in biodiesel production.

Table 12 Fatty acid composition in biomass of cells cultured in medium under different conditions at day 7

Fatty acid	Carbon atom: double bond	Percentage of fatty acid in relation to total fatty acid	
		Control media	Optimized media
Myristic acid	C14:0	0.41± 0.1	ND
Palmitic acid	C16:0	36.22 ± 3.3 [a]	31.63 ± 0.06 [b]
Palmitoleic acid	C16:1	13.69 ± 1.48 [a]	17.27 ± 0.63 [b]
Heptadecanoic	C17:1	1.84 + 0.26 [a]	1.85 ± 0.08 [a]
Oleic acid	C18:1 n-9 cis	15.05 ± 2.87 [a]	9.33 ± 0.11 [b]
Linoleic acid	C18:2 n-6 cis	16.56 ± 2.08 [a]	25.83 ± 0.01 [b]
Linolenic acid	C18:3 n-3	1.21 ± 0.35 [a]	6.46 ± 0.40 [b]
Unidentified		15.02	7.63

ND = Not detected

Means within lines with different superscript letters are significantly different at $p \leq 0.05$

Table 13 Comparison of fatty acid compositions of *Synechococcus* sp. and other feedstocks

Feedstocks	Fatty acid composition (wt.%)										References
	C16:0	C16:1	C18:1	C18:2	C18:3	S	MU	PU	TUS	DU	
Synechococcus sp. (optimal)	31.63	17.27	9.33	25.83	6.46	31.63	28.45	32.29	60.74	93.03	Present study
Chlorella vugaris	25.1	2.1	16	44.3	6.3	25.1	18.1	55.6	73.7	129.3	(Lam & Lee, 2013)
Euglena sp.	42.05	3.35	1.09	22.22	22.98	48.88	4.45	46.66	51.11	97.77	(Mahapatra, Chanakya, & Ramachandra , 2013)
Sunflower	6.2	0.1	25.2	63.1	0.2	6.2	25.3	63.3	88.6	151.9	
Olive	11.6	1.0	75.0	7.8	0.6	15.6	76.0	8.4	84.4	92.8	(Ramos *et al*., 2009)
Soy bean	11.3	0.1	24.9	53.0	6.1	15.3	25.6	59.1	84.7	143.8	
Palm	36.7	0.1	46.1	8.6	0.3	44.7	46.4	8.9	55.3	64.2	

S = saturated fatty acid MU = mono-unsaturated fatty acid PU = poly-unsaturated fatty acid
TUS = total unsaturated fatty acid DU = degree of unsaturation

4.9. Transcription analysis of *GPAT* in *Synechococcus* sp. under optimized conditions

Changes in GPAT gene expression were identified by comparing biomass obtained under optimal conditions to those obtained under normal conditions. After 10 days of cultivation in BG-11 culture medium, *Synechococcus* sp. was transferred to optimal medium consisting of 10.62 mg L^{-1} NH_4Cl. Samples were then cultured for 48 h and 72 h, after which the relative expression values were obtained using the $^{\Delta\Delta}$Ct method, with *rnpB* as the internal reference gene. The highest transcript levels occurred in 48 h, when they were 2.87 fold greater than in the control, after which they declined **(Figure 12)**. Similarly, Yokoi *et al*. (1998) reported that expression of Arabidopsis GPAT resulted in increased levels of unsaturated fatty acids in transgenic rice compared to wild type. Overexpression of GPAT in the transgenic marine diatom, *Phaeodactylum tricornutum*, resulted in higher unsaturated fatty acids compared to wild type (Niu *et al*., 2016). Moreover, recombinant expression of GPAT was found to

enhance increased TAG production in the transgenic green microalga, *Chlamydomonas reinhardtii* (Iskandarov *et al*., 2016). Thus, the altered content of unsaturated fatty acids in these organisms was due to the activity of overexpressed GPAT.

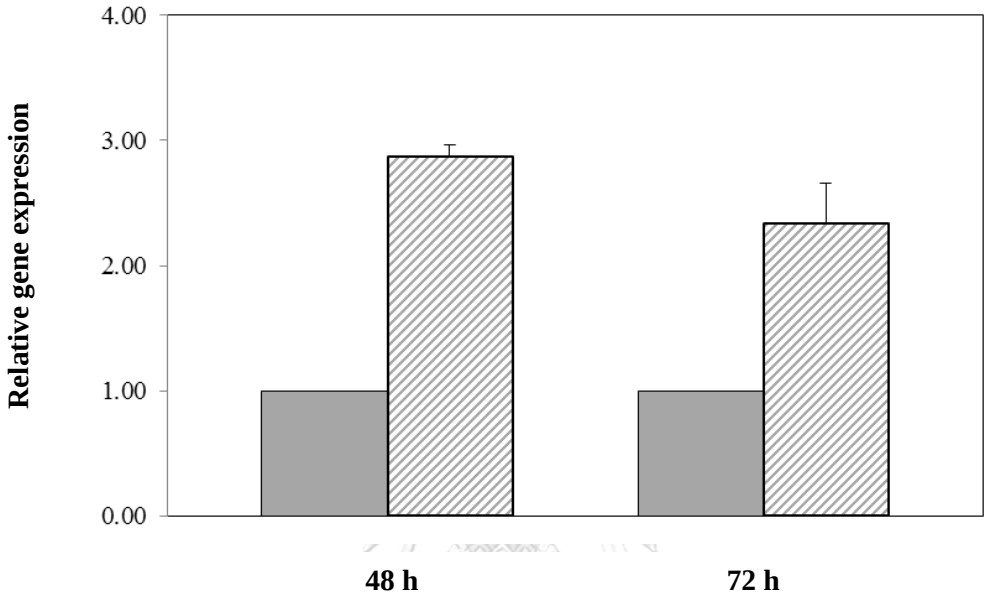

Figure 13 Expression of *GPAT* gene in *Synechococcus* sp. measured by qPCR; rnpB was used as a control gene. (▩) cells under the control medium (▨) cell under the optimal medium. Each value represents mean ±SD (n=3)

CHAPTER V
CONCLUSION

The results from the present study indicate that *Synechococcus* sp. was capable of growing and assimilating ammonium in medium supplemented with NH_4Cl at concentrations ranging from 1–10 mg N L^{-1}, but the growth was suppressed when the ammonium concentration was higher than 20 mg N L^{-1}. Ammonium can be assimilated by two different pathways, the activation of which depends on the concentration. Our analysis of GS and GOGAT revealed that both specific enzyme activity and *glnA*/*gltB* transcription were regulated in response to nitrogen availability. GS and GOGAT activity was rapidly down-regulated under excess ammonium concentrations, while GDH activity and *gdhA* transcription were up-regulated. Conversely, under optimal ammonium concentrations, the GS-GOGAT cycle becomes the major nitrogen assimilation process. Finally, we can conclude that marine cyanobacterium *Synechococcus* sp. is a suitable choice for improving the quality of saline aquaculture effluent. Moreover, using microalgae in terms of biofuel feedstock and water treatment seen in this study clearly indicates that the optimal state calculated by RSM was suitable for dual propose. The predicted value agreed well with the experimental value, as determined by validation experiments, which confirmed the availability and accuracy of the model. Under optimal condition, the highest ammonium removal and biomass production were obtained about 90% and 75.5% increasing, respectively within 7 day. The fatty acid profiles of *Synechococcus* sp. present high levels of saturated and monounsaturated fatty acids which together comprised more than 60% of the total fatty acids. Especially, large amount of palmitic acid may positive correlation with cetane number. Similarly with previous study, the expression of GPAT gene under optimal condition was significantly up-regulated compared to normal condition, which related to increasing of unsaturated fatty acids. Finally, it was concluded that using wastewater contaminated with ammonium as a nitrogen sources under

optimal condition is somewhat beneficial for this microalgae production to enhance biodiesel production.

REFERENCES

Ahmad, I., & Hellebust, J. A. (1990). Regulation of chloroplast development by nitrogen source and growth conditions in a Chlorella protothecoides strain. *Plant physiology, 94*(3), 944-949.

Allen, E. D., & Gorham, P. R. (1981). Culture of planktonic cyanophytes on agar *The Water Environment* (pp. 185-192): Springer.

Allen, S., & Smith, J. (1986). Ammonium nutrition in Ricinus communis: Its effect on plant growth and the chemical composition of the whole plant, xylem and phloem saps. *Journal of experimental botany, 37*(11), 1599-1610.

Altun, Ş. (2014). Effect of the degree of unsaturation of biodiesel fuels on the exhaust emissions of a diesel power generator. *Fuel, 117*, 450-457.

APHA/AWWA/WEF. (2005). Standard Methods for the Examination of Water & Wastewater: Centennial Edition: American Public Health Association New York.

Arbib, Z., Ruiz, J., Álvarez-Díaz, P., Garrido-Perez, C., & Perales, J. A. (2014). Capability of different microalgae species for phytoremediation processes: Wastewater tertiary treatment, CO2 bio-fixation and low cost biofuels production. *Water Research, 49*, 465-474.

Azam, M. M., Waris, A., & Nahar, N. (2005). Prospects and potential of fatty acid methyl esters of some non-traditional seed oils for use as biodiesel in India. *Biomass and bioenergy, 29*(4), 293-302.

Bates, R. G., & Bower, V. E. (1956). Alkaline solutions for pH control. *Analytical Chemistry, 28*(8), 1322-1324.

Bezerra, M. A., Santelli, R. E., Oliveira, E. P., Villar, L. S., & Escaleira, L. A. (2008). Response surface methodology (RSM) as a tool for optimization in analytical chemistry. *Talanta, 76*(5), 965-977.

Borowitzka, M. A. (1998). Limits to growth *Wastewater treatment with algae* (pp. 203-226): Springer.

Boyle, N. R., Page, M. D., Liu, B., Blaby, I. K., Casero, D., Kropat, J., . . . Karpowicz, S. J. (2012). Three acyltransferases and nitrogen-responsive regulator are implicated in nitrogen starvation-induced triacylglycerol accumulation in Chlamydomonas. *Journal of Biological Chemistry, 287*(19), 15811-15825.

Bradford, M. M. (1976). A rapid and sensitive method for the quantitation of microgram quantities of protein utilizing the principle of protein-dye binding. *Analytical biochemistry, 72*(1-2), 248-254.

Brenchley, J. E., & Magasanik, B. (1974). Mutants of Klebsiella aerogenes lacking glutamate dehydrogenase. *Journal of bacteriology, 117*(2), 544-550.

Caicedo, J., Van der Steen, N., Arce, O., & Gijzen, H. (2000). Effect of total ammonia nitrogen concentration and pH on growth rates of duckweed (Spirodela polyrrhiza). *Water Research, 34*(15), 3829-3835.

Cao, J., Li, J.-L., Li, D., Tobin, J. F., & Gimeno, R. E. (2006). Molecular identification of microsomal acyl-CoA: glycerol-3-phosphate acyltransferase, a key enzyme in de novo triacylglycerol synthesis. *Proceedings of the National Academy of Sciences, 103*(52), 19695-19700.

Chávez, S., Lucena, J., Reyes, J., Florencio, F., & Candau, P. (1999). The presence of glutamate dehydrogenase is a selective advantage for the cyanobacterium Synechocystis sp. strain PCC 6803 under nonexponential growth conditions. *Journal of bacteriology, 181*(3), 808-813.

Chen, B., Li, F., Liu, N., Ge, F., Xiao, H., & Yang, Y. (2015). Role of extracellular polymeric substances from Chlorella vulgaris in the removal of ammonium and orthophosphate under the stress of cadmium. *Bioresource technology, 190*, 299-306.

Coleman, R. A., & Mashek, D. G. (2011). Mammalian triacylglycerol metabolism: synthesis, lipolysis, and signaling. *Chemical reviews, 111*(10), 6359-6386.

Dahiya, A., Todd, J. H., & McInnis, A. (2012). Wastewater treatment integrated with algae production for biofuel *The Science of Algal Fuels* (pp. 447-466): Springer.

Dinarvand, M., Rezaee, M., Masomian, M., Jazayeri, S. D., Zareian, M., Abbasi, S., & Ariff, A. B. (2013). Effect of C/N ratio and media optimization through response surface methodology on simultaneous productions of intra-and extracellular inulinase and invertase from Aspergillus niger ATCC 20611. *BioMed research international, 2013*, 1-13.

Ebeling, J. M., & Timmons, M. B. (2012). Recirculating aquaculture systems. *Aquaculture production systems*, 245-277.

Einicker-Lamas, M., Mezian, G. A., Fernandes, T. B., Silva, F. L. S., Guerra, F., Miranda, K., . . . Oliveira, M. M. (2002). Euglena gracilis as a model for the study of Cu2+ and Zn2+ toxicity and accumulation in eukaryotic cells. *Environmental pollution, 120*(3), 779-786.

EPPO. (2016). Energy Situation in year 2015 and trend in year 2016. *Ministry of Energy, Thailand, http://www.eppo.go.th*.

Feng, Y., Li, C., & Zhang, D. (2011). Lipid production of Chlorella vulgaris cultured in artificial wastewater medium. *Bioresource technology, 102*(1), 101-105.

Gidda, S. K., Shockey, J. M., Rothstein, S. J., Dyer, J. M., & Mullen, R. T. (2009). Arabidopsis thaliana GPAT8 and GPAT9 are localized to the ER and possess distinct ER retrieval signals: functional divergence of the dilysine ER retrieval motif in plant cells. *Plant physiology and biochemistry, 47*(10), 867-879.

Gilmour, S. G. (2006). Response surface designs for experiments in bioprocessing. *Biometrics, 62*(2), 323-331.

González-Delgado, Á.-D., & Kafarov, V. (2011). Microalgae based biorefinery: Issues to consider. *CT&F-Ciencia, Tecnología y Futuro, 4*(4), 5-22.

Groat, R. G., & Vance, C. P. (1981). Root nodule enzymes of ammonia assimilation in alfalfa (Medicago sativa L.): developmental patterns and response to applied nitrogen. *Plant physiology, 67*(6), 1198-1203.

Guihéneuf, F., Leu, S., Zarka, A., Khozin-Goldberg, I., Khalilov, I., & Boussiba, S. (2011). Cloning and molecular characterization of a novel acyl-CoA: diacylglycerol acyltransferase 1-like gene (PtDGAT1) from the diatom Phaeodactylum tricornutum. *The FEBS journal, 278*(19), 3651-3666.

Gupta, A., & Sainis, J. K. (2010). Isolation of C-phycocyanin from Synechococcus sp.,(Anacystis nidulans BD1). *Journal of applied phycology, 22*(3), 231-233.

Harwood, J. L., & Guschina, I. A. (2013). Regulation of lipid synthesis in oil crops. *FEBS letters, 587*(13), 2079-2081.

Incharoensakdi, A., & Karnchanatat, A. (2003). Salt stress enhances choline uptake in the halotolerant cyanobacterium Aphanothece halophytica. *Biochimica et Biophysica Acta (BBA)-General Subjects, 1621*(1), 102-109.

Inokuchi, R., Kuma, K. i., Miyata, T., & Okada, M. (2002). Nitrogen-assimilating enzymes in land plants and algae: phylogenic and physiological perspectives. *Physiologia Plantarum, 116*(1), 1-11.

Iskandarov, U., Sitnik, S., Shtaida, N., Didi-Cohen, S., Leu, S., Khozin-Goldberg, I., . . . Boussiba, S. (2016). Cloning and characterization of a GPAT-like gene from the microalga Lobosphaera incisa (Trebouxiophyceae): overexpression in Chlamydomonas reinhardtii enhances TAG production. *Journal of applied phycology, 28*(2), 907-919.

Iwai, M., Ikeda, K., Shimojima, M., & Ohta, H. (2014). Enhancement of extraplastidic oil synthesis in Chlamydomonas reinhardtii using a type-2 diacylglycerol acyltransferase with a phosphorus starvation–inducible promoter. *Plant biotechnology journal, 12*(6), 808-819.

Jain, R., Coffey, M., Lai, K., Kumar, A., & MacKenzie, S. (2000). Enhancement of seed oil content by expression of glycerol-3-phosphate acyltransferase genes: Portland Press Limited.

Kennedy, E. P. (1961). *Biosynthesis of complex lipids.* Paper presented at the Fed. Proc.

Knothe, G., Matheaus, A. C., & Ryan III, T. W. (2003). Cetane numbers of branched and straight-chain fatty esters determined in an ignition quality tester☆. *Fuel, 82*(8), 971-975.

Koroleff, F. (1983). *Determination of ammonia* (Grasshoff & M. E. a. F. Kremling Eds.): John Wiley & Sons.

Lam, M. K., & Lee, K. T. (2013). Effect of carbon source towards the growth of Chlorella vulgaris for CO2 bio-mitigation and biodiesel production. *International Journal of Greenhouse Gas Control, 14*, 169-176.

Lea, P. J., & Miflin, B. J. (2003). Glutamate synthase and the synthesis of glutamate in plants. *Plant physiology and biochemistry, 41*(6-7), 555-564.

Lepage, G., & Roy, C. C. (1986). Direct transesterification of all classes of lipids in a one-step reaction. *Journal of lipid research, 27*(1), 114-120.

Lewin, T. M., Wang, P., & Coleman, R. A. (1999). Analysis of amino acid motifs diagnostic for the sn-glycerol-3-phosphate acyltransferase reaction. *Biochemistry, 38*(18), 5764-5771.

Li, H., Yang, W., Zhou, D., & Yu, W. (2018). Numerical study of the effects of biodiesel unsaturation on combustion and emission characteristics in diesel engine. *Applied Thermal Engineering, 137*, 310-318.

Lim, S.-L., Chu, W.-L., & Phang, S.-M. (2010). Use of Chlorella vulgaris for bioremediation of textile wastewater. *Bioresource technology, 101*(19), 7314-7322.

Limanond, T., Jomnonkwao, S., & Srikaew, A. (2011). Projection of future transport energy demand of Thailand. *Energy policy, 39*(5), 2754-2763.

Liu, B., & Benning, C. (2013). Lipid metabolism in microalgae distinguishes itself. *Current opinion in biotechnology, 24*(2), 300-309.

Livak, K. J., & Schmittgen, T. D. (2001). Analysis of relative gene expression data using real-time quantitative PCR and the 2− ΔΔCT method. *methods, 25*(4), 402-408.

Mahapatra, D. M., Chanakya, H., & Ramachandra, T. (2013). Euglena sp. as a suitable source of lipids for potential use as biofuel and sustainable wastewater treatment. *Journal of applied phycology, 25*(3), 855-865.

McNeely, K., Xu, Y., Bennette, N., Bryant, D. A., & Dismukes, G. C. (2010). Redirecting reductant flux into hydrogen production via metabolic engineering of fermentative carbon metabolism in a cyanobacterium. *Applied and environmental microbiology, 76*(15), 5032-5038.

Mérida, A., Candau, P., & Florencio, F. J. (1991). Regulation of glutamine synthetase activity in the unicellular cyanobacterium Synechocystis sp. strain PCC 6803 by the nitrogen source: effect of ammonium. *Journal of bacteriology, 173*(13), 4095-4100.

Miflin, B. J., & Habash, D. Z. (2002). The role of glutamine synthetase and glutamate dehydrogenase in nitrogen assimilation and possibilities for improvement in the nitrogen utilization of crops. *Journal of experimental botany, 53*(370), 979-987.

Morris, I. (1974). Nitrogen assimilation and protein synthesis *Algal physiology and biochemistry* (Vol. 10, pp. 583-609): Blackwell Oxford.

Myers, R. H., Montgomery, D. C., Vining, G. G., Borror, C. M., & Kowalski, S. M. (2004). Response surface methodology: a retrospective and literature survey. *Journal of quality technology, 36*(1), 53.

Neori, A., Chopin, T., Troell, M., Buschmann, A. H., Kraemer, G. P., Halling, C., . . . Yarish, C. (2004). Integrated aquaculture: rationale, evolution and state of the art emphasizing seaweed biofiltration in modern mariculture. *Aquaculture, 231*(1-4), 361-391.

Niazi, A., Khorshidi, N., & Ghaemmaghami, P. (2015). Microwave-assisted of dispersive liquid–liquid microextraction and spectrophotometric determination of uranium after optimization based on Box–Behnken design and chemometrics methods. *Spectrochimica Acta Part A: Molecular and Biomolecular Spectroscopy, 135*, 69-75.

Niu, Y.-F., Wang, X., Hu, D.-X., Balamurugan, S., Li, D.-W., Yang, W.-D., . . . Li, H.-Y. (2016). Molecular characterization of a glycerol-3-phosphate acyltransferase reveals key features essential for triacylglycerol production in Phaeodactylum tricornutum. *Biotechnology for biofuels, 9*. doi: https://doi.org/10.1186/s1306801604781

Niu, Y.-F., Zhang, M.-H., Li, D.-W., Yang, W.-D., Liu, J.-S., Bai, W.-B., & Li, H.-Y. (2013). Improvement of neutral lipid and polyunsaturated fatty acid biosynthesis by overexpressing a type 2 diacylglycerol acyltransferase in marine diatom Phaeodactylum tricornutum. *Marine drugs, 11*(11), 4558-4569.

Paulo, F., & Santos, L. (2017). Design of experiments for microencapsulation applications: A review. *Materials Science and Engineering: C, 77*, 1327-1340.

Perez-Garcia, O., Escalante, F. M., de-Bashan, L. E., & Bashan, Y. (2011). Heterotrophic cultures of microalgae: metabolism and potential products. *Water Research, 45*(1), 11-36.

Pham, M., Schideman, L., Scott, J., Rajagopalan, N., & Plewa, M. J. (2013). Chemical and biological characterization of wastewater generated from hydrothermal liquefaction of Spirulina. *Environmental science & technology, 47*(4), 2131-2138.

Pulz, O., & Gross, W. (2004). Valuable products from biotechnology of microalgae. *Applied microbiology and biotechnology, 65*(6), 635-648.

Ramesh, S., Muthuvelayudham, R., Rajesh Kannan, R., & Viruthagiri, T. (2013). Enhanced production of xylitol from corncob by Pachysolen tannophilus using response surface methodology. *International journal of food science, 2013*, 1-8.

Ramos, M. J., Fernández, C. M., Casas, A., Rodríguez, L., & Pérez, Á. (2009). Influence of fatty acid composition of raw materials on biodiesel properties. *Bioresource technology, 100*(1), 261-268.

Ruffing, A. M. (2014). Improved free fatty acid production in cyanobacteria with Synechococcus sp. PCC 7002 as host. *Frontiers in bioengineering and biotechnology, 2*, 17.

Sanjaya, M., Rachel, Durrett, T. P., Kosma, D. K., Lydic, T. A., Muthan, B., Koo, A. J., . . . Ohlrogge, J. (2013). Altered lipid composition and enhanced nutritional value of Arabidopsis leaves following introduction of an algal diacylglycerol acyltransferase 2. *The Plant Cell, 25*(2), 677-693.

Sara, G. (2007). Ecological effects of aquaculture on living and non-living suspended fractions of the water column: a meta-analysis. *Water Research, 41*(15), 3187-3200.

Sawaengsak, W., Silalertruksa, T., Bangviwat, A., & Gheewala, S. H. (2014). Life cycle cost of biodiesel production from microalgae in Thailand. *Energy for Sustainable Development, 18*, 67-74.

Shapiro, B., & Stadtman, E. (1970). The regulation of glutamine synthesis in microorganisms. *Annual Reviews in Microbiology, 24*(1), 501-524.

Skopelitis, D. S., Paranychianakis, N. V., Paschalidis, K. A., Pliakonis, E. D., Delis, I. D., Yakoumakis, D. I., . . . Roubelakis-Angelakis, K. A. (2006). Abiotic stress generates ROS that signal expression of anionic glutamate dehydrogenases to form glutamate for proline synthesis in tobacco and grapevine. *The Plant Cell, 18*(10), 2767-2781.

Sonani, R. R., Patel, S., Bhastana, B., Jakharia, K., Chaubey, M. G., Singh, N. K., & Madamwar, D. (2017). Purification and antioxidant activity of phycocyanin from Synechococcus sp. R42DM isolated from industrially polluted site. *Bioresource technology, 245*, 325-331.

Steinberg, D. M., & Kenett, R. S. (2014). Response surface methodology. *Encyclopedia of Statistics in Quality and Reliability*.

Takagi, M., & Yoshida, T. (2006). Effect of salt concentration on intracellular accumulation of lipids and triacylglyceride in marine microalgae Dunaliella cells. *Journal of bioscience and bioengineering, 101*(3), 223-226.

Tsai, A.-Y., Gong, G.-C., Chung, C.-C., & Huang, Y.-T. (2018). Different impact of nanoflagellate grazing and viral lysis on Synechococcus spp. and picoeukaryotic mortality in coastal waters. *Estuarine, Coastal and Shelf Science*.

USDA. (2017). Thailand Biofuel Annual 2017. *Global Agricultural Information Network, USDA Foreign Agricultural Service*.

Vassilev, S. V., & Vassileva, C. G. (2016). Composition, properties and challenges of algae biomass for biofuel application: an overview. *Fuel, 181*, 1-33.

Wan, L., Han, J., Sang, M., Li, A., Wu, H., Yin, S., & Zhang, C. (2012). De novo transcriptomic analysis of an oleaginous microalga: pathway description and gene discovery for production of next-generation biofuels. *PloS one, 7*(4), e35142.

Wang, T., Ge, H., Liu, T., Tian, X., Wang, Z., Guo, M., . . . Zhuang, Y. (2016). Salt stress induced lipid accumulation in heterotrophic culture cells of Chlorella protothecoides: mechanisms based on the multi-level analysis of oxidative response, key enzyme activity and biochemical alteration. *Journal of biotechnology, 228*, 18-27.

Witek-Krowiak, A., Chojnacka, K., Podstawczyk, D., Dawiec, A., & Pokomeda, K. (2014). Application of response surface methodology and artificial neural network methods in modelling and optimization of biosorption process. *Bioresource technology, 160*, 150-160.

Xu, J., Zheng, Z., & Zou, J. (2009). A membrane-bound glycerol-3-phosphate acyltransferase from Thalassiosira pseudonana regulates acyl composition of glycerolipids. *Botany, 87*(6), 544-551.

Zhang, W., Zhao, Y., Cui, B., Wang, H., & Liu, T. (2016). Evaluation of filamentous green algae as feedstocks for biofuel production. *Bioresource technology, 220*, 407.

Zou, J., Katavic, V., Giblin, E. M., Barton, D. L., MacKenzie, S. L., Keller, W. A., . . . Taylor, D. C. (1997). Modification of seed oil content and acyl composition in the Brassicaceae by expression of a yeast sn-2 acyltransferase gene. *The Plant Cell, 9*(6), 909-923.

APPENDIX

APPENDIX A

Culture medium and reagents preparation

1. BG-11 Turks Island salt solution medium

1.1 Stock BG-11 (100x)

$NaNO_3$	149.50	g
$MgSO_4 \cdot 7H_2O$	7.48	g
$CaCl_2 \cdot 2\ H_2O$	3.60	g
Citric acid	0.60	g
Na_2EDTA	0.104	g

Adjusted volume to 1 L with deionized water

1.2 Stock A (10x)

KCl	6.66	g
$MgCl_2 \cdot 6H_2O$	55.00	g
$CaCl_2 \cdot 2\ H_2O$	14.66	g

Adjusted volume to 1 L with deionized water

1.3 Stock B (10x)

$MgSO_4 \cdot 7H_2O$	74.80	g

Adjusted volume to 1 L with deionized water

1.4 Trace element (1000x)

H_3BO_3	2.86	g
$MnCl_2 \cdot 4H_2O$	1.81	g
$ZnSO_4 \cdot 7H_2O$	0.22	g
$NaMoO_4 \cdot 2H_2O$	0.39	g

$CuSO_4 \cdot 5H_2O$	0.08	g
$Co(NO_3)_2 \cdot 6H_2O$	0.05	g
KH_2PO_4	30.50	g
Ferric ammonium citrate	6.00	g
Na_2CO_3	20.00	g

Adjusted volume to 1 L with deionized water

To prepare BG-11 medium combine the following stock solutions:

Stock solution	Per Liter of medium	
Stock BG-11 (100x)	10	mL
Stock A (10x)	100	mL
Stock B (10x)	100	mL
Trace element (1000x)	1	mL

Adjusted volume to 1 L with deionized water

2. Preparation of Tris-HCl buffer (Bates & Bower, 1956)

To create 1000 ml of a 0.05 M Tris-HCl buffer, mix 50 mL solution A and x mL solution B as given below. Adjust to pH 8

Solution A: 0.05 M Tris hydrochloride

Solution B: 0.05 M HCl

pH	B (mL)
7.3	42.0
7.4	40.3
7.5	38.5
7.6	36.6
7.7	34.5
7.8	32.0
8.0	29.2
8.1	26.2
8.2	22.9
8.3	19.9
8.4	17.2
8.5	14.7
8.6	12.4
8.7	10.3
8.8	8.5
8.9	7.0
9.0	5.7

3. Bradford solution and protocol

3.1 Bradford stock solution

95% Ethanol	100	mL
88% Phosphoric acid	200	mL
SERVA Blue G	350	mg

3.2 Bradford working buffer

Bradford stock solution	30	mL
Deionized water	425	mL
95% Ethanol	15	mL
88% Phosphoric acid	30	mL

Note: Before using, Bradford working buffer must be filtered through the Whatman No.1 paper. Bradford working buffer is kept in a brown glass bottle at room temperature.

Bradford's protocol:

1. Pipette 60 µL of sample into 1.5 mL microtube.
2. Add 600 µL of Bradford working buffer and mix this solution.
3. Pipette 200 µL of this solution into 96-well plates.
4. Shake and read and absorbance at 595 nm after 2 min.

4. The reagent for glutamine synthetase (GS) assay and protocol

Reagent:

A. Imidazole-HCl buffer, 1 M pH 7: dissolve 6.81 g of imidazole in 80 mL of distilled water, adjust to pH 7 with 4 N HCl and diluted with distilled water to 100 mL.

B. ATP solution, 0.12 M: dissolve 0.726 g of ATP·Na_2·$3H_2O$ in 8 ml of distilled water, adjust to pH 7.0 with 1 N NaOH and dilute with distilled water to 10 mL.

C. L-Glutamate solution, 2.0 M: dissolve 37.4 g of sodium L-glutamate in 80 ml of distilled water, adjust to pH 7.0 with 1 N NaOH and dilute with distilled water to 100 mL.

D. NH_4Cl solution, 1.0 M: dissolve 5.35 g of NH_4Cl in 100 ml of distilled water.

E. $MgCl_2$ solution, 1.67 M: dissolve 34.0 g of $MgCl_2 \cdot 6H_2O$ in 100 mL of distilled water.

F. $FeSO_4$ solution, 29 mM: dissolve 0.8 g of $FeSO_4 \cdot 7H_2O$ in 100 mL of 0.3 N H_2SO_4 (prepare freshly).

G. Ammonium molybdate reagent, 53 mM: dissolve 6.6 g of $(NH_4)_6Mo_7O_{24} \cdot 4H_2O$ in 100 mL of 7.5 N H_2SO_4.

Protocol: 1. Prepare the following reaction mixture.

1.0 mL Imidazole–HCl buffer	(Reagent A)
2.5 mL ATP solution	(Reagent B)
2.0 mL L-Glutamate solution	(Reagent C)
1.0 mL NH_4Cl solution	(Reagent D)
0.6 mL $MgCl_2$ solution	(Reagent E)
2.9 mL Distilled water	

2. Pipette 0.2 mL of the reaction mixture and 0.1 mL of distilled water in a test tube.

3. Equilibrate at 37°C for about 5 min.

4. Add 0.1 mL of sample and incubate for 10 min at 37°C.

5. Add 1.8 ml of $FeSO_4$ solution (Reagent F) to stop the reaction, and then add 0.15 mL of ammonium molybdate reagent (Reagent G).

6. Read the absorbance at 660 nm in a cuvette (light path: 1 cm) (A_S). The blank solution is prepared by reversing the sequence of the addition of sample and $FeSO_4$ solution (Reagent F) (A_0).

Definition of unit: One unit (U) is defined as the amount of enzyme which produces 1 μmol of phosphate per min.

5. The reagent for glutamate synthase (GOGAT) and glutamate dehydrogenase (GDH) assay and protocol

Reagent:

A. Tris HCl 50 mM

Dissolve 60.7 g Tris base in 800 mL H_2O Adjust to desired pH with concentrated HCl Mix (as mention above) and add of distilled water to 1000 mL.

B. 200 mM 2-oxoglutarate (MW = 146.11): dissolve 0.292 g 2-oxoglutarate in 10 mL of distilled water.

C. 200 mM L-glutamine (MW = 146.14): dissolve 0.292 g L-glutamine in 10 mL of distilled water.

D. 50 mM $MgSO_4 \cdot 7H_2O$ (MW = 246.47): dissolve 0.123 g $MgSO_4$ 7 H_2O in 10 mL of distilled water.

E. 2.5 mM NADH (MW = 709.40): dissolve 1 mg NADH in 564 μL of distilled water.

F. NH_4Cl solution, 1.0 M: dissolve 5.35 g of NH_4Cl in 100 ml of distilled water.

Protocol (GOGAT):

1. Prepare the following reaction mixture.

5 mL Tris HCl buffer (Reagent A)

1 mL 20 mM 2-oxoglutarate (Reagent B)

1 mL 20 mM L-glutamine (Reagent C)

1 mL 5 mM $MgSO_4$ (Reagent D)

1 mL 0.25 mM NADH (Reagent E)

2. Pipette 0.9 mL of the reaction equilibrates at 45°C for about 5 min.

3. Add 0.1 mL of sample and incubate for 10 min at 37°C

4. The production or consumption of NADH was monitored at 340 nm for 4 min.

Definition of unit: One unit (U) is defined as the amount of enzyme needed to consume 1 μmol NADH per minute under the conditions described above.

Protocol (GDH):

1. Prepare the following reaction mixture.

5 mL Tris HCl buffer pH 8 (Reagent A)

1 mL 50 mM 2-oxoglutarate (Reagent B)

1 mL 0.25 mM NADH (Reagent C)

1 mL 10 mM $MgSO_4$ (Reagent D)

1 mL 100 mM NH_4Cl (Reagent E)

2. Pipette 0.9 mL of the reaction equilibrates at 45°C for about 5 min.

3. Add 0.1 mL of sample and incubate for 10 min at 37°C

4. The production or consumption of NADH was monitored at 340 nm for 4 min.

Definition of unit: One unit (U) is defined as the amount of enzyme needed to consume 1 μmol NADH per minute under the conditions described above.

APPENDIX B

Standard curve for determine the protein concentration by Bradford method

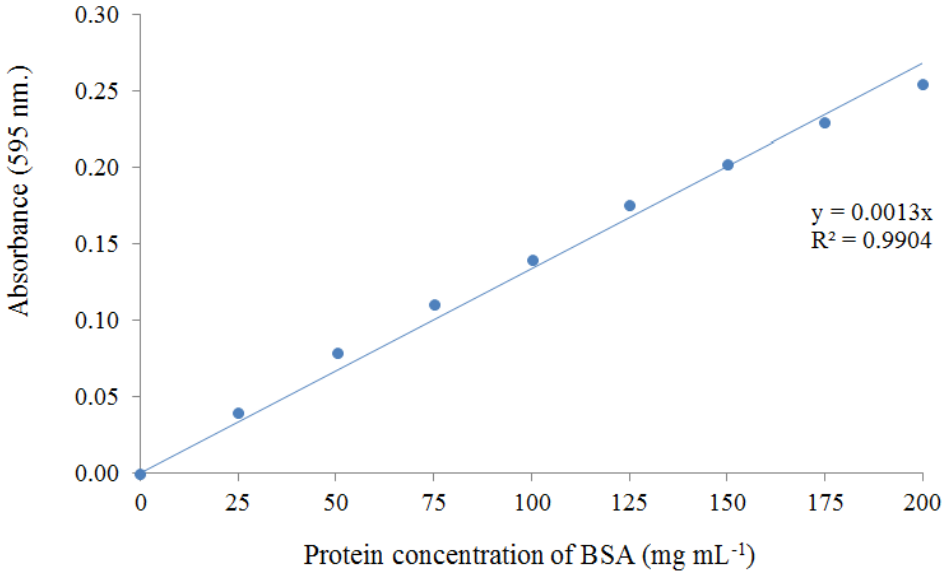

Standard curve for determine phosphate concentration

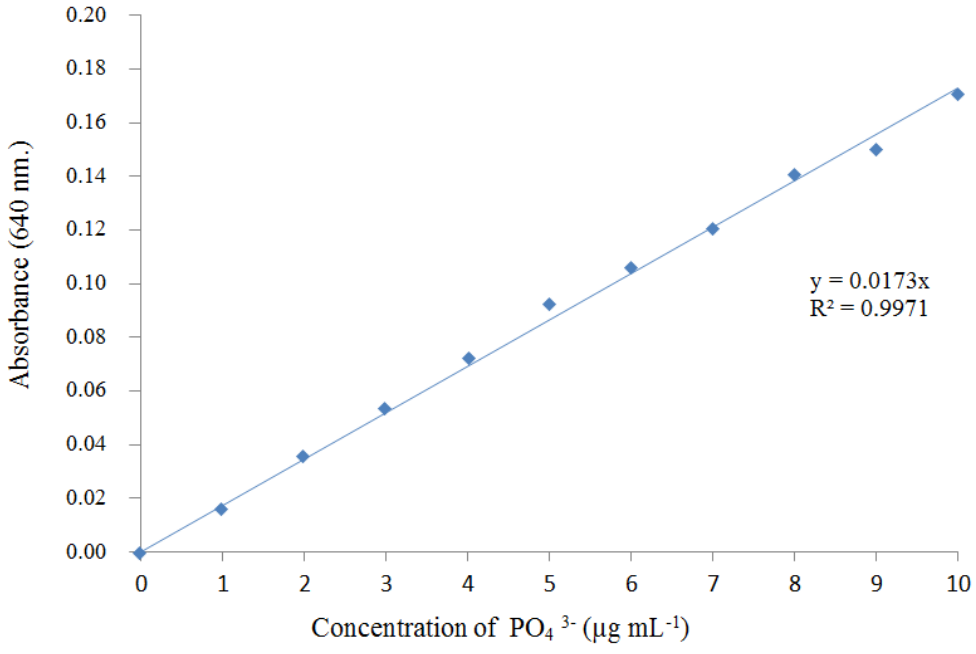

Standard curve for determine NADH concentration

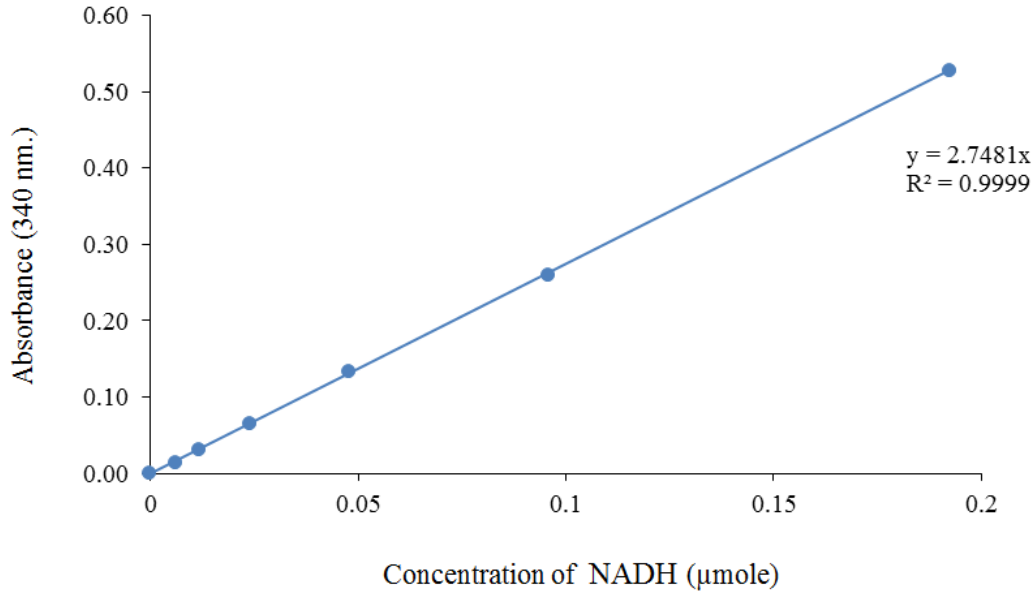

Standard curve for determine ammonium concentration

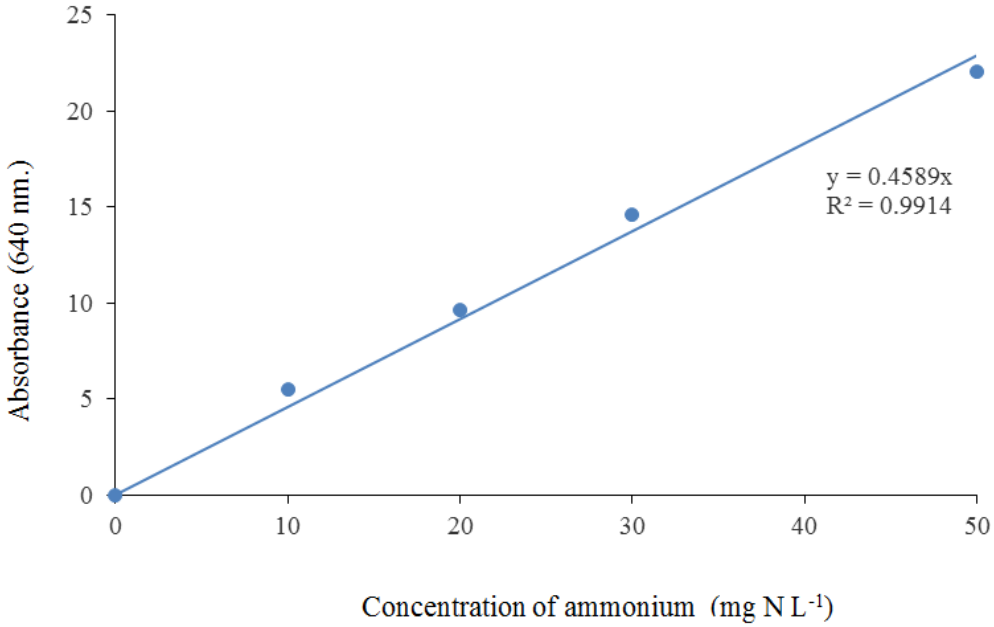

(a)

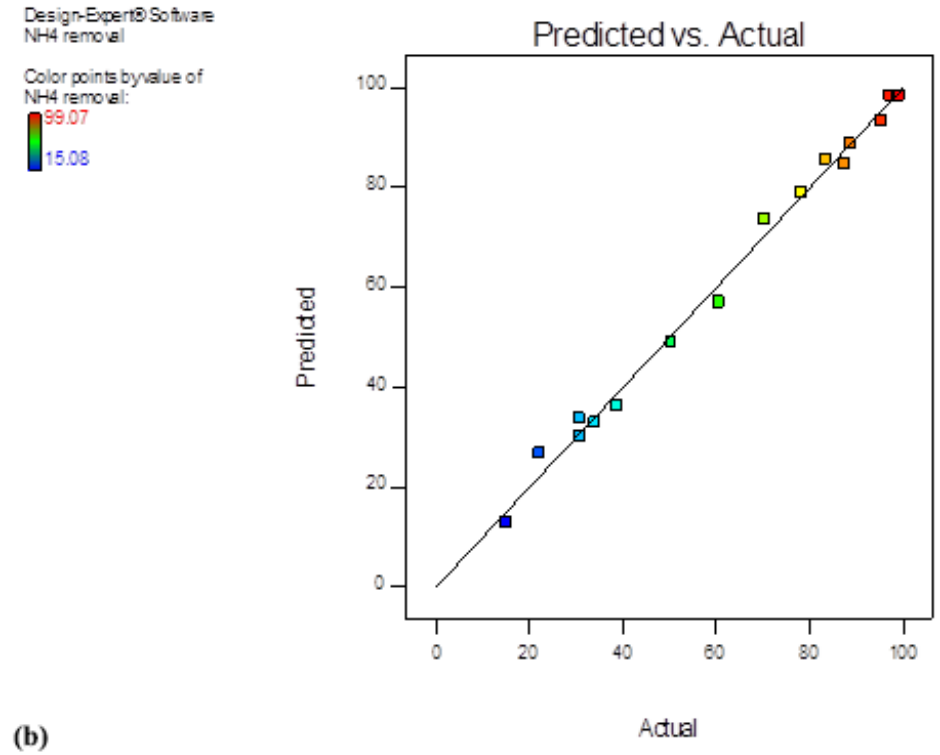
Design-Expert® Software
NH4 removal
Color points by value of
NH4 removal:
99.07
15.08
Predicted vs. Actual
Predicted
Actual
0
20
40
60
80
100

(b)

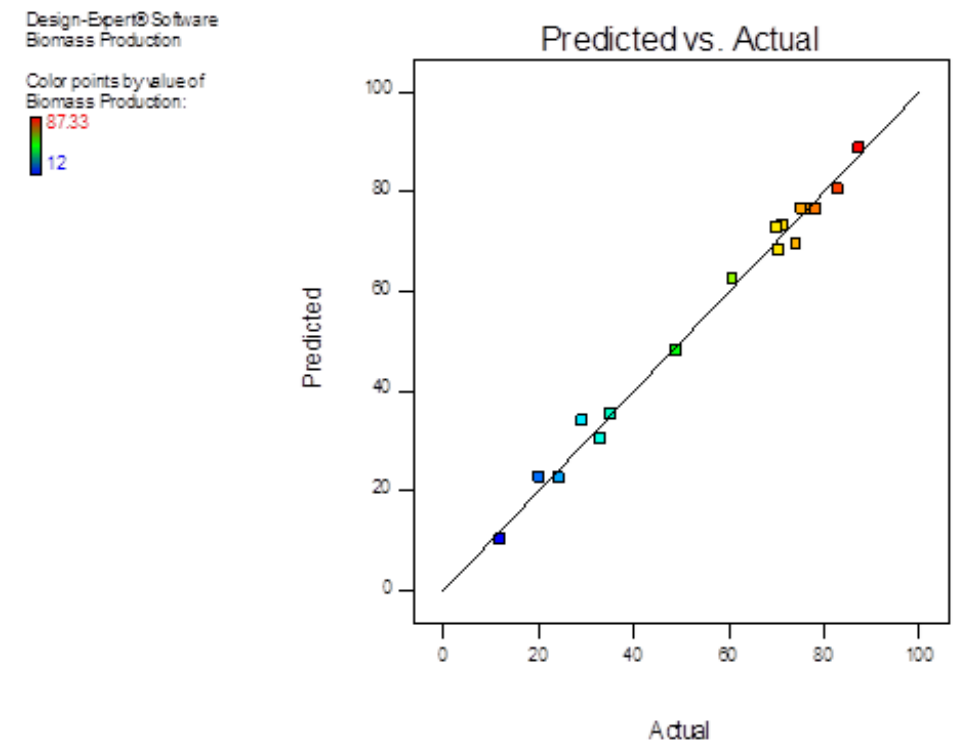
Design-Expert® Software
Biomass Production
Color points by value of
Biomass Production:
87.33
12
Predicted vs. Actual
Predicted
Actual
0
20
40
60
80
100

VITA

Miss Piroonporn Srimongkol was born on January 13, 1982 in Chantaburi, Thailand. In 2003, she received a Bachelor's degree of Science in Biology from Prince of Songkla University and then worked as a lecturer at Rajamangala University of Technology Tawan-ok Chanthaburi Campus. In 2005, she decided to enter master's degree programs of Biotechnology, Faculty of Science, King Mongkut's Institute of Technology Ladkrabang and completed her master degree in 2009. After that, she started doctoral degree in Program of Biotechnology, Faculty of Science, Chulalongkorn University under the supervision of Associate Professor Dr. Aphichart Karnchanatat.

Academic presentations;

1. Srimongkol, P., Tongchul, N., Phunpruch, S. and Karnchanatat, A. 2016. Effect of ammonium stress on growth, key enzyme activities and ammonium assimilation of cyanobacterium Synechococcus sp. VDW. The 5th International Biochemistry and Molecular Biology Conference: Biochemistry for a sustainable future, 26-27th May 2016, B.P. Samila Beach Hotel, Songkhla, Thailand.

2. Srimongkol, P., Tongchul, N., Phunpruch, S. and Karnchanatat, A. 2017. Application of response surface methodology (RSM) for ammonium removal and biomass production from artificially prepared shrimp wastewater by Synechococcus sp VDW. The 7th International Conference on Fermentation Technology for Value Added Agricultural Products and The 12th Asian Biohydrogen & Biorefinery Symposium, 25– 28th July 2017, Pullman Khon Kaen Raja Orchid Hotel, Khon Kaen, Thailand